

A communication efficient distributed learning framework for smart environments

Lorenzo Valerio^{a,*}, Andrea Passarella^a, Marco Conti^a

^a*Institute of Informatics and Telematics, National Research Council, Via Moruzzi 1, Pisa. Italy*

Abstract

Due to the pervasive diffusion of personal mobile and IoT devices, many “smart environments” (e.g., smart cities and smart factories) will be, among others, generators of huge amounts of data. To provide value-add services in these environments, data will have to be analysed to extract knowledge. Currently, this is typically achieved through centralised cloud-based data analytics services. However, according to many studies, this approach may present significant issues from the standpoint of data ownership, and even wireless network capacity. One possibility to cope with these shortcomings is to move data analytics closer to where data is generated. In this paper we tackle this issue by proposing and analysing a distributed learning framework, whereby data analytics are performed at the *edge* of the network, i.e., on locations very close to where data is generated. Specifically, in our framework, *partial* data analytics are performed directly on the nodes that generate the data, or on nodes close by (e.g., some of the data generators can take this role on behalf of subsets of other nodes nearby). Then, nodes exchange partial models and refine them accordingly. Our framework is general enough to host different analytics services. In the specific case analysed in the paper we focus on a learning task, considering two distributed learning algorithms. Using an activity recognition and a pattern recognition task, both on reference datasets, we compare the two learning algorithms between each other and with a central cloud solution (i.e., one that has access to the complete datasets). Our results show that using distributed machine learning techniques, it is possible to drastically reduce the network overhead, while obtaining performance comparable to the cloud solution in terms of learning accuracy. The analysis also shows when each distributed learning approach is preferable, based on the specific distribution of the data on the nodes.

Keywords: Iot, big data, smart cities, distributed learning, communications efficiency

1. Introduction

1.1. Motivation

The massive diffusion of personal mobile and IoT devices is one of the propellers behind many “smart environments” where pervasive networking and computing technologies are increasingly applied. The sheer number of devices predicted to be installed in smart environments is impressive, commonly considered in the order of billions or trillions by 2025, resulting in a density of about 1000 devices per person all over the world [1]. Perhaps even more importantly, each of these devices is a data generator, and their pervasive diffusion means that huge amounts of data will be generated at the *edge* of the network, where these devices will reside. According to Cisco, also as a side effect of the pervasive diffusion of personal mobile and IoT devices, the global mobile data traffic will increase at an exponential pace. It will increase nearly eightfold between 2015 and 2020, at a compound annual growth rate (CAGR) of 53%, reaching 30.6 exabytes per

*Corresponding authors

Email addresses: l.valerio@iit.cnr.it (Lorenzo Valerio), a.passarella@iit.cnr.it (Andrea Passarella), m.conti@iit.cnr.it (Marco Conti)

month by 2020 [2]. This data traffic increase is typically referred to as the *data tsunami*. These data once properly processed, open uncountable possibilities in terms of novel applications and services. Data and knowledge extracted from data is indeed the “glue” bonding together the physical part of a smart environment (e.g., the physical infrastructures of a city, such as lighting, heating, traffic control, water distribution, smart grids, and, extensively, people) and its cyber part (i.e., the Internet services based on its data). The continuous interaction between the cyber and the physical parts, mediated by data, enables not only to sense the status of the physical environment, but also to act upon it based on the knowledge extracted from data. This is at the basis of the Cyber-Physical convergence concept [3] for pervasive environments.

According to current IoT/M2M paradigms [4, 5, 6], the typical workflow adopted to process and extract knowledge from data is based on central cloud systems. Precisely, to extract knowledge from raw data, typical IoT/M2M architectures (e.g., the ETSI M2M architecture [7]) consider three main layers. In the first layer gateways collect data from individual “things”. In the second layer, data is sent to the central cloud via some pervasive (wireless) network infrastructure, such as LTE. In the third layer, knowledge is extracted from data and provided to applications or further exploited to create new services.

Although such IoT/M2M architecture has proved to be very powerful in current applications, it may have significant shortcomings in the medium term. First, it assumes the presence of a very broadband wireless access network to move data from the collection to the processing layers. Unfortunately, even the adoption of the latest 4G LTE-A technologies might not provide sufficient capacity in the medium term [8, 9, 10]. Right now we are in the early adoption phase of 4G technologies, which is giving a significant boost to the cellular capacity with respect to the current demands. However, projections over the next years show that this additional capacity may be saturated soon and may not be sufficient to cope with the data tsunami effect [2]. As a consequence, bandwidth crunch events similar to those occurred with 3G networks [11] may be expected, unless alternative solutions are devised in time. Second, collecting all data in a central place might not be always feasible due to privacy or ownership constraints [12]. This applies both to general personal devices of users, who might not be willing to give away data about their personal behaviour, but also to many “verticals” such as industrial environments, where significant fractions of the data would have to remain local to specific production environments [13].

One possibility to cope with these problems is to limit the amount of data sent to global cloud platforms, and move part or the data processing tasks to the edge of the network, where data is generated. This is the vision of (Mobile) Edge Computing [14], Fog computing [15], and opportunistic computing [16]. Not only this approach can help offloading excessive traffic from wireless access networks. It can indeed be the most suitable approach to extract knowledge also from privacy sensitive data, which may not be transferred to third parties (global cloud operators) for processing [14]. Note that this approach is gaining more and more momentum both in the research and industry environments. For example, Google has recently advertised a mobile computing framework, called Federated Learning [17]. In Federated Learning, mobile devices (smartphones or tablet) spread all over the world, collaborate to perform a deep learning task and learn a global model from their local data. All the learning phases are incrementally accomplished directly on the data owned locally by devices, and data is never sent to the cloud.

This approach can be applied to multiple instances of smart environments. One example are smart factories, where data about the production process, collected either by sensors or by operators devices, need to be analysed to understand the status of the production, in order to dynamically tune or even reconfigure the processes. This is the typical case considered in the Industry 4.0 (or Industrial Internet) framework [18]. In most of the cases, industries are not willing to move their data to some external cloud provider infrastructure, due to confidentiality reasons. On the other hand, they will not have the competences to build and manage a private cloud platform. In this case, decentralised analytics solutions where data are directly analysed on the devices available on the factory premises will have several advantages. It will avoid leaking of information outside of the factory environment, and will reduce the dependency and cost of IT services provided by external IT operators [13]. Another use case for distributed analytics are more general smart cities services. For instance, think to a mobile crowd sensing scenario in which people located in a limited geographical area (e.g. a park, square, museum, etc.) are performing some activity, and their smart devices have to infer collectively what, either single users or the whole crowd, is doing. Privacy issues may restrict the transmission of data to a central cloud [19]. Moreover, most of the time analytics

computed over these data may be relevant only for limited time span and at very specific locations, making movement of data back and forth the devices in those locations a complete waste of bandwidth. This is the scenario for which several localised mobile social networking applications have recently been created (e.g., Here&Now [20], Crowd-Cache [21]). In this context, additional trust and incentives issues may arise, which are typically not present in smart factory environments (or other environments where the set of devices is under the ownership of a single or a federation of operators). For example, users would need to be incentivised to perform data analytics on behalf of each other, and they need to trust the results computed by the others.

1.2. Contribution

In this paper we focus on the mobile crowd sensing scenario, and we target the general problem of extracting knowledge through machine learning techniques from a dataset that is collected across a number of physical locations, and available at distinct mobile nodes, one per location¹. We define a framework where learning is mostly performed locally at each individual location, and the amount of information to be shared across locations is minimised. Precisely, in our case we compute partial models built on the local datasets and our purpose is to come up with a more refined model that includes the knowledge of all the partial models, while minimising the amount of information exchanged between nodes that compute the partial models.

We focus on two real learning cases, and use reference datasets in the literature. The first one is about activity recognition from data sampled by smart-phones in individual locations. The second one is about digits recognition. Note that the main purpose of the datasets is to show, with reference benchmarks the validity of the proposed distributed learning approach, more than providing specific use cases for smart cities scenarios. As a matter of fact, the first dataset serves also the latter role. It is, in fact, representative of cases where users' personal devices need to recognise activities that are contextualised to the specific behaviour of their users in specific locations, possibly for limited amounts of time. In these cases, recognising the activity of each individual user by monitoring exclusively its own behaviour (a typical activity recognition task which can be implemented at each node in isolation) may not be meaningful, as the activities would be specific to the location and context of the user during a certain time window. It is more useful to derive activity recognition models from a multitude of users who would behave approximately the same because they share the same context for a certain time. There are a few important remarks bound to this scenario. The first one is related to data labelling. We point out that in this paper we focus on the definition and evaluation of the learning framework, assuming that data held by phones has been already labelled either by the user or other mechanisms. Manual tagging for collected data such as in the activity recognition example would not be totally uncommon in these contexts. A second remark is related to incentives for users to collaborate in the distributed task, and trust mechanisms by which users can trust the partial models computed by others. Both problems are very relevant, but they are common to several crowd sensing systems. In this paper we consider them mostly as orthogonal problems. Note, however, that in the paper we analyse the robustness of our scheme to malicious behaviours, and we show that the proposed scheme is able to automatically filter out maliciously modified partial models. This property, together with dedicated mechanisms, can help in addressing trust issues.

As in our prior work [22], in this paper we use a distributed learning algorithm based on the Hypothesis Transfer Learning (HTL) scheme proposed in [23]. The algorithm we use trains a separate model for each location where part of the dataset is available, exchanges partial models between locations, and finally obtains a unique refined model. In this paper, we significantly extend our prior work in several directions. We consider a set of different distributed learning models, in addition to HTL. We contrast the prediction performance of all the schemes between each other, and with respect to a centralised solution where all data is sent to a central cloud platform. Specifically, we compare all schemes in terms of prediction performance and network overhead. Our results show that, in general all distributed solutions achieve prediction accuracies

¹Indeed, in the following we will use the concept of physical location and mobile node storing data collected at that location interchangeably.

very close to the centralised cloud solution. Depending on the scenario and the distribution of data on the nodes, different distributed learning approaches yield the best trade-off between accuracy and network traffic. However, in all cases, the best distributed approach yields accuracy comparable with a centralised solution, while drastically cutting the network traffic, between 52% and up to 99%. We also derive analytical bounds on this gain, and analyse its sensitiveness with respect to the key involved parameters. Moreover, we compare the distributed solutions in terms of the trade off between network traffic and prediction performance. In general, HTL outperforms simpler solutions in terms of prediction by generating higher network traffic. Therefore, we define a modified HTL solution where traffic is drastically reduced, without compromising the prediction performance. In addition, we evaluate the performance of all the distributed solutions in presence of malicious users, which inject wrong partial models in the system. We show that, contrarily to other distributed algorithms, HTL is very robust in this case, as nodes are able to automatically filter out corrupted partial models. Finally, we analyse the performance of the distributed algorithms in dynamic scenarios, where nodes come and go dynamically over time, and participate to the learning task during different time intervals. We show that also in this case distributed algorithms can achieve very high accuracy with a drastic reduction of network traffic. All in all, we think that these results provide a strong validation on the viability of distributed data analytics schemes at the edge of the network. In the paper we consider learning problems, i.e., a very specific instance of data analytics, to have a practical case to work with. However, the framework we propose is more general, and can accommodate any data analytics problem for which distributed algorithms are available.

The rest of the paper is organised as follows. Section 2 presents related work. Section 3 provides a brief background on HTL, which is then applied to our problem in Section 4. Sections 5 describe the datasets we have used. Section 6 compares the distributed solutions with each other and with the cloud-based solution. Section 7 shows the robustness of HTL to malicious behaviour of devices. Section 8 analyses the network traffic overhead, while Section 9 shows how to further optimise the trade-off between traffic overhead and prediction accuracy for HTL. Section 10 analyses the performance of the distributed learning algorithms in dynamic conditions. Finally, Section 11 concludes the paper.

2. Related work

The distributed learning problem could be approached in many ways. One possibility is represented by “ensemble methods” such as bagging, boosting and mixtures of experts [24, 25, 26, 27]. Intuitively, these methods allocate portions of the training dataset to different classifiers that are independently trained. The individual classifiers are subsequently aggregated, sometimes through a different training algorithm and sometimes using feedback from the training phase of the individual classifiers. These approaches might be suitable for distributed learning in parallel networks, however they are generally designed within the classical model for supervised learning and fundamentally assume that the training set is available to a single coordinating processor.

Motivated by the presence of huge quantities of data, there are other machine learning techniques that focus on scaling up the typical centralized learning algorithm. One approach is to decompose the training set into smaller “chunks” and subsequently parallelize the learning process by assigning distinct processors/agents to each of the chunks. This is the typical scenario in which deep learning is widely used [28, 29, 30]. Differently from our solution, these approaches do not target knowledge extraction where data have privacy constraints, or when network overhead should be minimised.

Finally, other works propose fully distributed and decentralized learning algorithms. To the best of our knowledge, the more relevant with respect to our reference scenario are the following. In [31] authors present a distributed version of Support Vector Machine (SVM). In order to learn a model from physically distributed data, they propose an iterative procedure according to which they i) train an SVM on each local dataset and then they exchange the learned Support Vectors (i.e. relevant points of the dataset that determine the classifier) with all the other locations. These Support Vectors are added to each local dataset and the local SVMs are trained again. Authors of [32] propose a distributed learning algorithm for arbitrary connected machines. The approach consists of an initial learning phase performed on the local data and then an iterative consensus procedure through which machines come up with a final model. Another similar

solution presented in [33] propose two distributed learning algorithms for Random Vector Functional Link Networks (RVFL). The first one is based on a Decentralised Consensus Algorithm. The second one, instead, is based on the Alternative Direction Method of Multipliers. Both are iterative solutions that in order to converge to a model have to repeatedly exchange their partial models’ parameters. Other solutions belong the “stacked generalisation” family whose the typical approach is to learn a global model that combines the outputs of several partial models [34]. Precisely, in this approach every machine holds a local dataset that is split into training set and validation set. Each machine trains a local model on training set and share it with all the other locations. At each location all the received models are tested on the validation set and answers are sent to a unique collecting machine that trains a “meta-model” on this newly created dataset. This last trained model represents the final model. This approach is not suitable in our case because it would generate an amount of traffic that is proportional to the size of the validation sets at each location and to the number of locations.

All these solutions typically converge to a model whose accuracy is comparable with a centralized algorithm with access to the entire dataset. However, none of them consider the amount of network traffic triggered by their iterative procedures. In this paper, instead, we consider two state of the art ensemble learning approaches that are suitable to be trained without a complete “view” of the dataset and we compare their performance with a distributed learning solution based on Hypothesis Transfer Learning proposed in our previous paper [35]. It is worth noting that although it shares some similarity with the “stacking generalisation” paradigm, it does not send any data over the network. Moreover, for the sake of completeness we compare the performance of all the considered procedures with a centralised cloud-based benchmark, i.e. a learning algorithm that has complete access to the entire dataset at hand.

The main novelty and goal of this paper is not to champion one distributed learning approach over the others, but rather to perform a comparative study that highlights, in different working scenarios, their benefits. Our purpose, in the end, is to be able to select the best learning technique, in terms of accuracy and networks traffic, for different IoT scenario.

3. Hypothesis transfer learning

In this section we present the core part of the distributed learning solution based on Hypothesis Transfer Learning. Specifically, in this paper the general learning task we take into account is about classification. Therefore, the Hypothesis Transfer Learning approach we selected to build the distributed learning approach is a classification algorithm called GreedyTL [23].

For the sake of clarity, before providing the details of GreedyTL, we describe with a simple example a high level intuition about the general Hypothesis Transfer Learning framework. Let us consider the existence of one small dataset D_1 and two larger datasets D_2, D_3 collected across three separate locations and let us consider that these datasets are only locally accessible. Let us suppose that we already have learnt a model for both D_2 and D_3 , here denoted by h_2 and h_3 , respectively. Now we want to learn a model on D_1 , denoted by h_1 . Note that, since in machine learning the accuracy of a model strongly depends on the size of the dataset, the small size of D_1 will negatively affect the accuracy of h_1 . According to the HTL framework, in order to overcome this problem we can exploit the knowledge contained in h_2, h_3 to learn a more accurate model h_1 on the dataset D_1 . In the HTL terminology, the models h_2, h_3 are called *source models* while h_1 is called *target model*. Analogously, D_2, D_3 are referred as source domains and D_1 as target domain.

Let us now introduce the notation used in this section: small bold letters denote column vectors. The training set of cardinality m is denoted as the set of pairs $\{(\mathbf{x}_i, y_i)\}_{i=1}^m$ where $\mathbf{x}_i \subseteq \mathcal{X} \in \mathbb{R}^d$ and $y \subseteq \mathcal{Y} \in \mathbb{R}$. Here \mathcal{X}, \mathcal{Y} denote respectively the input and the output space of a learning problem. Here we denote with $\{h_i^{src}(\mathbf{x})\}_{i=1}^L$ the set of L source models and with h^{trg} the target model that we have to learn in the target domain.

GreedyTL focuses on the binary classification problem. However, it is worth noting that this is not a limitation because it can be easily extended to the multi-class classification problem (details about how we used it in a multi-class classification problem are provided in the next section). The model that GreedyTL learns is defined as follows:

$$h^{trg}(\mathbf{x}) = \boldsymbol{\omega}^T \mathbf{x} + \sum_{i=1}^L \beta_i h_i^{src}(\mathbf{x}) \quad (1)$$

Note that the target model is a standard linear classifier of the form

$$h^{trg}(\mathbf{x}) = \boldsymbol{\omega}^T \mathbf{x}$$

with an additional term

$$\sum_{i=1}^L \beta_i h_i^{src}(\mathbf{x})$$

that permits to include the knowledge of the source models into the target model. The β coefficients control how much each source model can affect the behaviour of the target model. Here $\boldsymbol{\omega}$ and $\boldsymbol{\beta}$ are the parameters of the target model to be learnt.

In order to find the best combination of parameter $\boldsymbol{\omega}$ and $\boldsymbol{\beta}$, GreedyTL solves the following optimization problem

$$\begin{aligned} (\boldsymbol{\omega}^*, \boldsymbol{\beta}^*) &= \operatorname{argmin}_{\boldsymbol{\omega}, \boldsymbol{\beta}} \left\{ \hat{R}(h^{trg}) + \lambda \|\boldsymbol{\omega}\|_2^2 + \lambda \|\boldsymbol{\beta}\|_2^2 \right\} \\ &\text{s.t. } \|\boldsymbol{\omega}\|_0 + \|\boldsymbol{\beta}\|_0 \leq \kappa \end{aligned} \quad (2)$$

The meaning of the objective function is the following. The first term

$$\hat{R}(h^{trg}) = \frac{1}{m} \sum_{i=1}^m (h^{trg}(\mathbf{x}_i) - y_i)^2$$

is the mean squared error and says that we are looking for linear classifier h^{trg} that minimises the number of prediction errors. The terms

$$\lambda \|\boldsymbol{\omega}\|_2^2 + \lambda \|\boldsymbol{\beta}\|_2^2$$

are called regularization terms, and their effect is to avoid to find a model that over-fits the data in the training set. This is called Tikhonov regularization and it is a common practice in the machine learning field to improve the generalisation capabilities of the learning algorithms [36]. Here λ is a parameter used to control the impact of this second term in the final solution of the optimization problem. Finally, the constraint of the optimization problem

$$\|\boldsymbol{\omega}\|_0 + \|\boldsymbol{\beta}\|_0 \leq \kappa$$

imposes that the number of non-null coefficients of the vectors $\boldsymbol{\omega}$ and $\boldsymbol{\beta}$, collectively do not exceed a constant parameter κ . In this way we force the algorithm to select only those source models that collectively improve the generalisation of the target model and, as a consequence, the size of the target model is limited. Summarising in this way we are looking for model of size at most κ , that minimises the prediction error.

It is important to note that the formulation of this optimisation problem is a special case of the Subset Selection problem [37] which aims at finding the subset of κ out of $d + L^2$ variables that maximises the prediction of a selected variable (such as the class label for a classification problem)[23]. However, as specified in [37] the subset selection problem is NP-hard, therefore we can only find an approximate solution. To this end the problem (2) is solved using a regularized Least Square Forward Regression algorithm that iteratively tests and adds features to the solution until the number of features added is $\leq \kappa$ and such that the prediction error is minimised.

As shown in [23], this algorithm is very accurate even with very small-sized training sets. From a computational point of view, the small size of the training set, however is a mandatory condition for GreedyTL

² $d + L$ is the sum of the sizes of the $\boldsymbol{\omega}$ and $\boldsymbol{\beta}$ vectors, respectively.

because it has to invert a matrix whose size is proportional to the size of the local dataset at hand, i.e. the matrix inversion operation is computationally very expensive. Since we want our procedure to be general, we cannot pose a limit on the size of the dataset. Therefore, we overcome this limitation in the following way. For each data location we train several instances of GreedyTL on different randomly drawn small samples of the local dataset and at the end we take the average of all this models. In this way, we are able to apply GreedyTL even to a big dataset. Moreover, this procedure can be easily parallelised on a multi core machine. As it will be clear in Section 6.1, this brings a strong impact on the generalisation performance³ of GreedyTL with respect to the performance of the local base model.

4. Distributed Learning procedures

In this section we define the distributed learning problem we cope with in this paper and the two distributed learning procedures we consider in our comparative study.

4.1. Problem description

In this paper we consider the following scenario. We assume that a dataset D is distributed over different devices located in a number L of different physical locations. Therefore each location l holds a partition $D_l, l = 1, \dots, L$ of D . Clearly, we assume that the data contained in each partition D_l are homogeneous, e.g., for a sensing application, they must be related to a well-defined physical entity that is sensed across different locations. This is necessary to meaningfully use, for the model corresponding to one partition, features of the models trained on the rest of the partitions.

In this paper, we assume that the partitions D_l are the training sets for training l partial classifiers, which are then refined based on each other features. Therefore, each local dataset is in the form $D_l = \{\mathbf{X}_l, \mathbf{Y}_l\}$ where $X_l \in \mathbb{R}^{n_l \times d}$ is the set of examples (or patterns) available at the l -th location l , $Y_l \in \mathbb{R}^{n_l \times 1}$ is the set of labels that define the class to which each pattern belongs to, n_l is the cardinality of D_l and d is the number of features of each pattern $\mathbf{x} \in \mathbf{X}$ (i.e., the dimensionality of each data point in the dataset). We consider that all that nodes can communicate between each others through the network. Specifically, instead of the data, they exchange the models they have learnt from their local datasets. Hereafter, according to the general machine learning terminology, with the term machine we identify a computationally capable device that has direct access to the local dataset in order to execute a learning procedure and learn a model of the data. Specifically, a machine is therefore a machine learning algorithm running at the node where the local dataset is stored. A model is a parametric function h that takes in input a pattern $\mathbf{x} \in \mathbf{X}$ and returns in output a number \hat{y} that corresponds to the class label to which the pattern \mathbf{x} belongs. The parameters of the function h are the quantities to be learnt by the machine learning algorithm.

4.2. GTL: Distributed learning through Hypothesis Transfer learning

Now we describe the distributed learning solution based on GreedyTL. It is composed of 5 steps that are performed by each machine. Algorithm 1 shows the pseudo-code of this algorithm.

Step 0 (Lines 1-5). In the first step each machine at each location trains a learner on its local data. Although in principle every learning algorithm could be used during this phase, in our paper we use a Linear Support Vector Machine learning algorithm [38]. It is worth noting that it is possible to adapt the same procedure to other learning algorithms but we have chosen this learning algorithm because of its well known good performance and simplicity. After this first learning step, each location l_i holds a model $h_{l_i}^{(0)}$ (Line 5).

Step 1 (Lines 6-8). After Step 0, there is the first synchronisation phase. All the models learnt at each location are sent to all the other locations. At the end of this phase each location holds L SVM linear predictors, each one trained on different data. Note that at every location, models are stored in the same order, i.e. $h_1^{(0)}$ is the same model at each location. As it will be clear later on this is instrumental to enable the second step of model aggregation described in Step 4.

³the performance of the algorithm applied to data not used during the training

Step 2 (Line 9). At each location we perform a second training phase on the same data using GreedyTL. To this end we provide to it the set of models obtained during the previous steps. The output of this step is the model defined in Equation 1. It is worth noting that the actual form of this model is a single vector $\omega' = [\beta^T, \omega^T]^T$ where the first L components correspond to the β coefficients and the rest to the ω coefficients. Note that its dimensionality is greater than the dimensionality of the problem, i.e. the problem has dimensionality d while ω' has dimensionality $d + L$. However, as it will become clear in Section 8 this does not represent an issue from the network traffic point of view because, thanks to the ability of selecting the most informative features of GreedyTL algorithm, the vector ω' tends to be sparse.

Step 3 (Lines 10-12). After each location l has its new model $h_l^{(2)}$, we have a new synchronisation phase in which, like for Step 1, every location sends its $h_l^{(2)}$ model to all the other locations.

Step 4 (Line 13). Once all the models have been received, each location aggregates all of them into a single model $h^{(4)}$. As for Step 0, this aggregation can be done in several ways. Since we are framing into a classification problem, in this paper we adopted the majority voting and a consensus approach. Majority Voting is a very common technique used to aggregate the predictions of many classifiers into one single response. Briefly, it selects the most frequent prediction as final response. In the consensus aggregation, instead, $h^{(4)} = \frac{1}{L} \sum_{l=1}^L \omega'_l$. Of course these are just an example of the several and more sophisticated techniques one could apply at this Step. Here we used them because of their simplicity and, as we will see in Section 6.1, good performance.

Algorithm 1 GTL Distributed Learning procedure

- 1: Let be L the number of data locations
 - 2: Let be l_i the ID of the i -th location and l_c the ID of the current location c .
 - 3: Let be $h^{(j)}$ the local model at step j
 - 4: Let be $\mathbf{X}_c, \mathbf{y}_c$ the training patter and training labels for location l_c , respectively
 - 5: $h_{l_c}^{(0)} = \text{TrainBaseLearner}(\mathbf{X}_c, \mathbf{y}_c)$
 - 6: $\text{SendModelToAll}(h_{l_c}^{(0)})$
 - 7: $H^{src} = \text{ReceiveBaseModels}();$
 - 8: $H^{src} \leftarrow H^{src} \cup \{h_{l_c}^{(0)}\}$
 - 9: $h_{l_c}^{(2)} = \text{GreedyTL}(\mathbf{X}_c, \mathbf{y}_c, H^{src})$
 - 10: $\text{SendModelToAll}(h_{l_c}^{(2)})$
 - 11: $H^{gtl} = \text{ReceiveGTLModels}()$
 - 12: $H^{gtl} \leftarrow H^{gtl} \cup \{h_{l_c}^{(2)}\}$
 - 13: $h^{(4)} = \text{CombineModels}(H^{gtl})$
-

4.3. noHTL: Consensus and Majority Voting based distributed learning

Let us now introduce an alternative distributed learning procedure that we used in our comparative study with GTL. As a matter of fact, these procedures are a subset of the steps composing the GTL procedure. The main difference between GTL and noHTL is the absence of the second training phase, i.e., Steps 2 and 3 of GreedyTL. There is, moreover, a difference in the case when Majority Voting or Consensus-based aggregation is used. In the former case, at each location, the outcome is the most selected class by all the local models. Therefore, all models need to be available at all locations. From an algorithmic standpoint, therefore, noHTL with Majority Voting is exactly the same as GTL with the exclusion of steps 2 and 3, i.e., Lines 9-12 of Algorithm 1. On the other hand, in case of Consensus-based aggregation it is possible to optimise the algorithm to reduce the network overhead. Specifically, we assume that, instead of sending all models computed at Step 1 to all other nodes, they are sent to a unique node, which we call models collector. This node computes the average of the models, and sends this back to all the other nodes. Therefore, the steps of the algorithm become as follows, captured in Algorithm 2.

Step 0 (Lines 1-5). In the first step each machine at each location trains a learner on its local data as in the GTL procedure. For the sake of comparison we used the same base learner as for GTL.

Step 1 (Line 6-8). After Step 0 all the models learnt at each location are sent to one device that acts as models collector. It is not important which device is selected as models' collector. This is the first main difference with GTL. As we can see in the experimental part, this step has strong impact on the network traffic generated by this procedure.

Step 2 (Line 9). The model collector computes the average model similarly to Step 4 of the GTL procedure: $h^{(2)} = \frac{1}{L} \sum_{l=1}^L h_l^{(0)}$.

Step 3 (Lines 10-11). The model collector sends the mean model $h^{(2)}$ to all the other devices

Algorithm 2 noHTL Distributed Learning procedure

- 1: Let be L the number of data locations
 - 2: Let be l_i the ID of the i -th location and l_c the ID of the current location.
 - 3: Let be $h^{(j)}$ the local model at step j
 - 4: Let be \mathbf{X}, \mathbf{y} the training patten and training labels for location l_c , respectively
 - 5: $h_{l_c}^{(0)} = \text{TrainBaseLearner}(\mathbf{X}, \mathbf{y})$
 - 6: $\text{SendModelToAll}(h_{l_c}^{(0)})$
 - 7: $H^{src} = \text{ReceiveBaseModels}();$
 - 8: $H^{src} \leftarrow H^{src} \cup \{h_{l_c}^{(0)}\}$
 - 9: $h_{l_c}^{(2)} = \frac{1}{|H^{src}|} \sum_{l=1}^{|H^{src}|} h_l^{(0)}$.
 - 10: $\text{SendModelToAll}(h_{l_c}^{(2)})$
 - 11: $h^{(2)} = \text{ReceiveModel}()$
-

5. Datasets description

In this section we present the datasets we used to evaluate the considered solutions. We used two well known datasets containing real world measurements, the first one, the HAPT dataset, is commonly used in the field of Human Activity Recognition (HAR)[39], while the second one is the well-known MNIST dataset that contains images of handwritten digits [40]. Hereafter we provide a detailed description of both datasets.

5.1. HAPT dataset

The dataset was built during experiments carried out with a group of 30 volunteers within an age range of 19-48 years. Each volunteer performed a protocol of activities composed by six basic activities: three static postures (standing, sitting, lying) and three dynamic activities (walking, walking downstairs and walking upstairs). In the dataset are present also postural transitions that occurred between the static postures (e.g. stand-to-sit, sit-to-stand, sit-to-lie, lie-to-sit, stand-to-lie, and lie-to-stand). All the participants were wearing a smart-phone (Samsung Galaxy S II) on the waist during the experiment execution. The raw measurements are 3-axial linear acceleration and 3-axial angular velocity at a constant rate of 50Hz using the embedded accelerometer and gyroscope of the device. Afterwards, the sensor signals (accelerometer and gyroscope) were pre-processed by applying noise filters and then sampled in fixed-width sliding windows of 2.56 sec and 50% overlap (128 readings/window). From each window, a vector of 561 features was obtained by calculating variables from the time and frequency domain. The resulting dataset is composed by $N = 10929$ records where each one is a vector $x \in \mathbb{R}^d, d = 561$. The total size in MB of the raw measurements is 103MB that is greater than the size of the post-processed dataset (48MB). It is worth noting that, the distribution of activities for each user is skewed: static and dynamic postures are performed

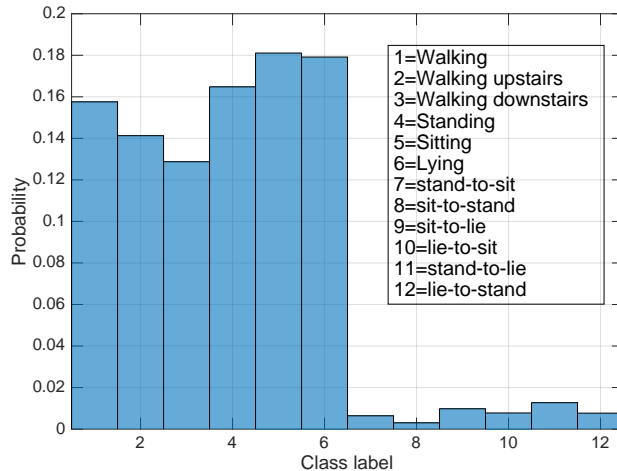


Figure 1: Probability density function of the activities performed by each user.

more frequently than transitions, as reported in Figure 1. Moreover, 9 local datasets out of 30 do not have a complete set of activities, therefore in our experiments we consider only those users that present a complete set of activities. The data corresponding to the excluded users have been uniformly distributed between the remaining 21 users. Note that the dataset is unbalanced, in the sense that different classes have quite different number of samples on which the models can be trained. As this is a critical point, we study in detail the behaviour of distributed learning in cases of various types of unbalanced datasets in Section 6.

5.2. MNIST dataset

MNIST is a database of 70000 handwritten digits. Images contained in the dataset are numbers from 0 to 9. Digits have been normalized and centered in a fixed size 28x28 image, meaning that each image in the dataset corresponds to a record of 784 raw features. As it is common practice when working with images, we transformed each one into a more informative feature set. Specifically, we transformed each image into a histogram oriented graph (HOG) [41]. The image is divided into a grid of small cells, and for the pixels within each cell, a histogram of gradient directions is computed, i.e. gradients are computed on the gray-scale value of pixels. The resulting HOG descriptor for an image is the concatenation of these histograms. In our experiments we used a cells grid of size 5×5 , meaning that the image is divided in 25 regions over which histograms are computed. After applying the HOG feature extraction method, each image is transformed into a feature vector of size 324. Note that this procedure is applied to each image separately therefore this workflow is perfectly compatible with a crowd sensing scenario like the one we are considering, i.e. pictures taken by users are preprocessed before being processed by our distributed learning system.

Similarly to the HAR scenario, we consider to have 30 users involved in a mobile crowdsourcing task in which each of them collects a certain number of images on their phones. In this paper we considered three possible scenarios. First, the classes distribution of digits per user is uniform, i.e. each user collected almost the same number of images per class (see Figure 2a). Second, the distribution of classes per user is equally skewed for all the users, i.e. for each device the classes of digits 2,5,6,7,8 are less represented than the others (see Figure 2b). Third, the classes distribution between users is different. Precisely, we simulated a “one hot” situation in which each user’s device collected many examples of one class and only few for the rest of the classes (see Figure 2c-2d). The most popular class is rotated among the 10 possible classes among the users, and thus each class is the most popular for 3 users.

The modifications in the second and third cases allow us to study a very important property of our proposed approach. Using these modifications of the MNIST dataset we are able to evaluate the performance of the proposed approach by unbalancing the dataset in a controlled way. Specifically, in the second case we

consider unbalancing between classes, but uniformity across locations, i.e., the number of data points are different across classes, but all locations “see” the same distribution of data points. This type of unbalancing (that is present also in the original HAPT dataset) is throughout referred to as “class unbalance”. In the third case the dataset is balanced across classes, but unbalanced across nodes, as different nodes “see” a different distribution of data points for training. This type of unbalance is throughout referred to as “node unbalance”. Note that one of the goals of GTL is to overcome unbalance of both types, by (i) transferring and refining knowledge obtained over limited-size datasets in case of class unbalance, and (ii) transferring knowledge acquired at locations with “more information” to locations with “less information” in case of node unbalance’. We anticipate that, as shown in Section 6, our GTL-based algorithm is able to achieve this goal.

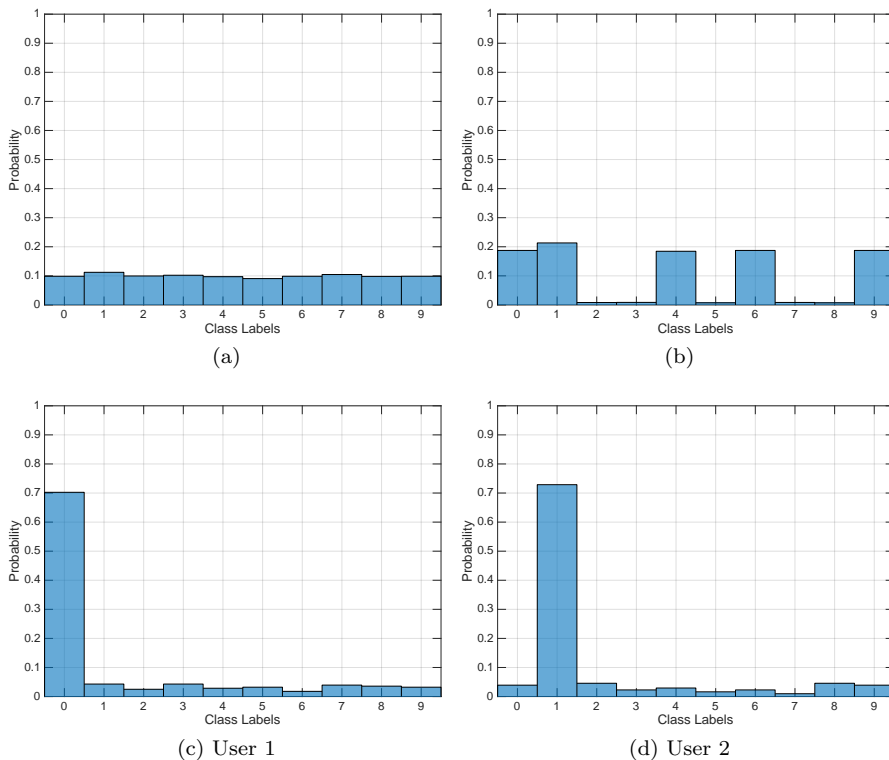


Figure 2: Per user class distribution for each MNIST-based dataset.

6. Results on prediction performance

We evaluate the performance of distributed learning using the two datasets in Sections 6.2 and 6.3, respectively. Sections 6.4 and 6.5 considers the case of MNIST with skewed distributions of samples, described in Section 5.

We recall that we compare the performance of GTL and noHTL to characterise the prediction performance vs. network overhead trade-off. We also compare them with a centralised solution where all data is sent to a central cloud (this approach is hereafter referred to as “Cloud”). Before presenting the results, in Section 6.1, we discussed the performance indices used in the analysis.

6.1. Performance metrics

In this paper we evaluate the prediction performance of our system using the well known F-measure [42]. The F-measure is a common aggregate index mostly used to evaluate the performance of a content retrieval

system or a classifier. We use it because it provides a more precise description of the performance of our system with respect to the simple accuracy index defined as the number of correct predictions divided by the total number of predictions made. Precisely, through the F-measure we are able to summarize in one single index the performance expressed by the Precision and Recall indexes. The F-measure is defined as the harmonic mean between the precision index and the recall index, hereafter defined. Note that in this paper all the performance indexes are location-wise, i.e. they always refer to performance obtained by models trained in each separate location l .

The precision (or specificity) index is defined as the number of correct predictions divided by the total number of predictions made. More formally:

$$p_l = \frac{1}{m_l} \sum_{i=1}^{m_l} I(y_i, \hat{y}_i) \quad (3)$$

with

$$I(y_i, \hat{y}_i) = \begin{cases} 1 & \text{if } y_i = \hat{y}_i \\ 0 & \text{otherwise} \end{cases}$$

where \hat{y} is the predicted class of the i -th pattern x_i and y_i is its true class and m is the number of the test set.

The recall (or sensitivity) index is defined as the number of correct predictions for a specific class divided by the number of the patterns that belong to that specific class, averaged over all classes. More formally:

$$r_l = \sum_{\forall c \in C} \frac{1}{m_{l,c}} \sum_{i=1}^{m_{l,c}} I(y_{c,i}, \hat{y}_{c,i}) \quad (4)$$

Finally the F-measure is defined as follows:

$$F_l = 2 * \frac{p_l \cdot r_l}{p_l + r_l} \quad (5)$$

This measure takes values in the range $[0, 1]$, where 0 stands for the worst prediction performance and 1 to the best one.

We define the Prediction Performance Gain (PPG) index as the percentage increment of prediction performance we gain after each step of both GTL and noHTL procedures, against the performance of the local base classifier, i.e. the local model learnt after Step 0. More formally, let us denote with $F_l^{h(0)}$ the F-measure value of the local model trained at Step 0 for location l and with $F_l^{h(j)}$ with $j > 1$ the model obtained at the j -th step. We compute the PPG gain $\rho_l^{(j)}$ at location l and step j as

$$\rho_l^{(j)} = 1 - \frac{1 - F_l^{h(j)}}{1 - F_l^{h(0)}} \quad (6)$$

As, in general, $1 - F$ is 1 when the classifier performs at worst, $\rho_l^{(j)}$ ranges from 0 and 1, and tends to 1 the more the various steps (specifically, steps 2 and 4 for GTL and noHTL with Majority Voting, Step 2 for noHTL with Consensus-based aggregation) improve performance with respect to step 0. Conversely, if ρ_l assumes a negative value, it means that the models obtained at the various steps are less accurate of the local base model.

We tested our framework adopting a “70-30” hold out procedure. Precisely, every round we keep the 30% of data as test set, and we apply our distributed learning procedure on the remaining 70%. Then the performance results are averaged over 10 runs and confidence intervals at 95% are computed. Note that for each run the data contained in the test set is never presented to learning algorithm during the training phase. We use it only to evaluate the performance of the model learnt at the end of the training phase.

Note that, the problem at hand falls in the domain of multi-class classification. The approach adopted in this paper to cope with more than two classes is the well-known “one-vs-all”. Specifically, here each

multi-class classifier is composed by k binary classifiers each one trained on its own class. For example, for the binary classifier corresponding to class 1, all the examples belonging to class 1 are treated as positive examples (labelled as +1) and the rest are negative examples (labelled as -1).

In order to decode the final response of the multi-class classifier we adopt the following standard approach. To each class label we associate a binary string of size k , e.g. if $k = 3$, the string associated to the class label $c = 2$ is $b_2 = \{-1, 1, -1\}$. When a pattern \mathbf{x} is presented to all the k trained binary learners, each of them provides its classification response (+1 or -1). Following the same example, all the classifiers' responses form a binary string \hat{b} , e.g. $\hat{b} = \{-1, 1, -1\}$ which, in this particular case means that the second classifier says that the pattern belongs to his own class, while the others say that the pattern does not belong to their own classes. The final response of the classifier corresponds to the class label corresponding to the binary string b_c that is more similar to the response string \hat{b} . More precisely:

$$\hat{y} = \operatorname{argmin}_{c \in \{1, \dots, k\}} \sum_{i=1}^k \max(0, 1 - \hat{b}[i] \cdot b_c[i])$$

where \hat{y} is the final response of the multi-class classifier, and $b[i]$ denotes the i -th element of string b .

6.2. Case study I: Human Activity Recognition (HAPT dataset)

Let us now present the performance related to the Activity Recognition dataset. We point out that the confidence intervals we obtained for all the results presented in this and the following Sections are very tight, therefore, we do not show them for the clarity of the plots.

Figure 3a shows the F-measure, in each data location, after each step of the proposed procedure. As one can expect, the local models trained at the Step 0 (here denoted for simplicity by $\text{GTL}^{(0)}$ but also valid in the $\text{noHTL}^{(0)}$, since both procedures have the same step 0), yield the worst performance. This is due to the fact that, although SVM is a very good learning algorithm, in the local data there are not enough examples to learn a model with good generalisation abilities. After the models' exchange at Step 1, we can see that the HTL algorithm is able to well exploit the knowledge learnt at each location and learn a model with better performance ($\text{GTL}^{(2)}$). Note that each $\text{GTL}^{(2)}$ model has been trained on the same local data on which was trained the $\text{GTL}^{(0)}$ models. After the second exchange of models, the performance of GTL are even better. Note that after the second exchange of models there are no more differences in terms of performance between the locations. This is due to the fact that at each location all the $\text{GTL}^{(2)}$ models learnt in all the other locations are aggregated into a single model ($\text{GTL}^{(4)}$), which is the same for all locations. In fact, looking at Figure 3a, we can see that the performance of the aggregated models based on HTL ($\mu\text{-GTL}^{(4)}$ and $mv\text{-GTL}^{(4)}$ stand for mean model and majority voting, respectively) get closer and closer to the performance obtained with a Cloud solution. In fact the F-measure with GTL is 0.95 while the one with the cloud approach is 0.995. As far as noHTL is concerned, we notice that in this specific case its performance in both variants is better than $\text{GTL}^{(0)}$, meaning that the model aggregation procedure is beneficial to improve the generalisation performance of each device. However, noHTL is not able to reach the GTL performance. As we see in the next set of results, this is due to the fact that noHTL is not able to compensate for insufficient representation of some classes (remember that the HAPT dataset is "class unbalanced"). A third interesting fact is that both $mv\text{-noHTL}$ and $\mu\text{-noHTL}$ have the same performance, reaching a final F-measure of 0.92.

In Figure 3b we show the performance gain of each step w.r.t. the performance of the local model. Specifically, for each step and each location we compute the corresponding performance gain. We sort locations in increasing order of loss of the local model $\text{GTL}^{(0)}$, and use this ordering in the x axis. In other words, the left-most values in the graph correspond to the gains obtained in the locations with the lowest F-measure of the base learner. Interestingly, the ranking shown in Figure 3a is preserved. In fact we notice that both GTL and noHTL improve the performance w.r.t. the local models. However in this scenario it is clear that simply averaging the local models is not enough to obtain good performance. It is also interesting to note that the gain of GTL solutions increases for locations where the local model performs worse. This means that, besides always improving over the local model, the HTL-based solution "helps more" the locations with a lower initial performance, which is also a desirable feature.

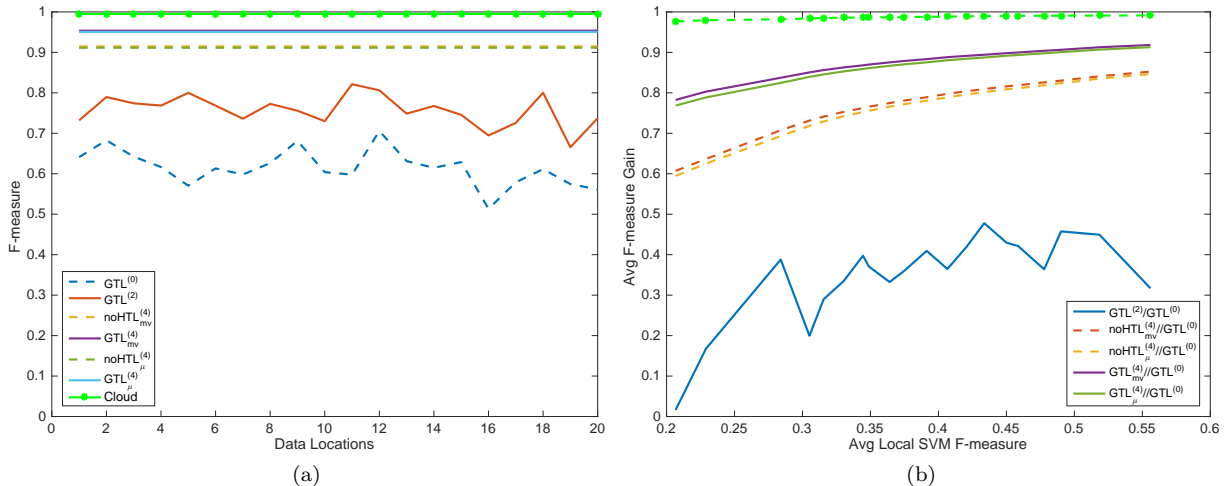


Figure 3: HAPT dataset. Prediction performance (a) and Prediction Performance Gain (b) comparison per single location after each step of the proposed distributed learning approach for both GTL and noHTL versions.

In order to understand the real benefit coming from the use of the considered distributed learning approaches, we analysed the accuracy per single class, averaged over all the locations for each step of each procedure. In this way we want to highlight that even though the labels’ distribution is unbalanced, there is an advantage in averaging local models (as both GTL and noHTL do), and that it is even more beneficial to transfer knowledge, as GTL does and noHTL does not. In fact, looking at Figure 4a we can notice that the unbalanced dataset strongly affects the performance of $GTL^{(0)}$ (remember from Figure 1 that classes 1 to 6 are way more represented in the dataset with respect to classes 7 to 12). With $GTL^{(2)}$, noHTL, and $GTL^{(4)}$ instead we notice an better performance. One reason behind it is that, in general, averaging local models reduces uncertainty and thus results in better performance. However, we clearly notice a difference in performance between $GTL^{(4)}$ and noHTL, due to the fact that GTL transfers knowledge across nodes. By doing so, it is able to aggregate knowledge obtained at individual locations over small datasets (for specific classes). This is supported by Figure 4b, which shows that GTL obtains a performance gain up to 80%. We point out that for the sake of clarity, we do not report the values for mv - $GTL^{(4)}$ because they are equal to the ones of μ - $GTL^{(4)}$.

6.3. Case Study II: Unmodified MNIST Dataset

In the case of the unmodified MNIST dataset, all location see the same distribution of data points per class, and all classes are equally represented. Therefore, there is no unbalance of any kind. Specifically, the distribution of classes in each local dataset owned by each device is of the form represented in Figure 2a.

Looking at Figures 5a-5b we notice that both noHTL and GTL yield very good performance, quite close to the one of the Cloud solution. As a matter of fact, in this case even local models are already quite good, due to the fact that classes are fairly well represented at each location. When comparing GTL and noHTL, it is interesting to note that noHTL outperforms GTL. The reason is that, as the dataset is totally balanced, aggregating local models (as noHTL does) is sufficient, while transferring knowledge may lead to over fitting, and sometimes even deteriorates performance with respect to local models (see Figure 5b). However, remember that our goal is not to champion GTL in all cases, but to show that distributed learning can be as efficient as cloud-based approaches. In this specific case, the best distributed learning solution is noHTL instead of GTL.

Figures 6a and 6b show the performance on a per-class basis. This analysis confirms the initial findings. In this case, as the dataset is balanced and all classes are already well represented at all locations, the advantage of transferring knowledge or aggregating local models is minimal, if any. Local models already

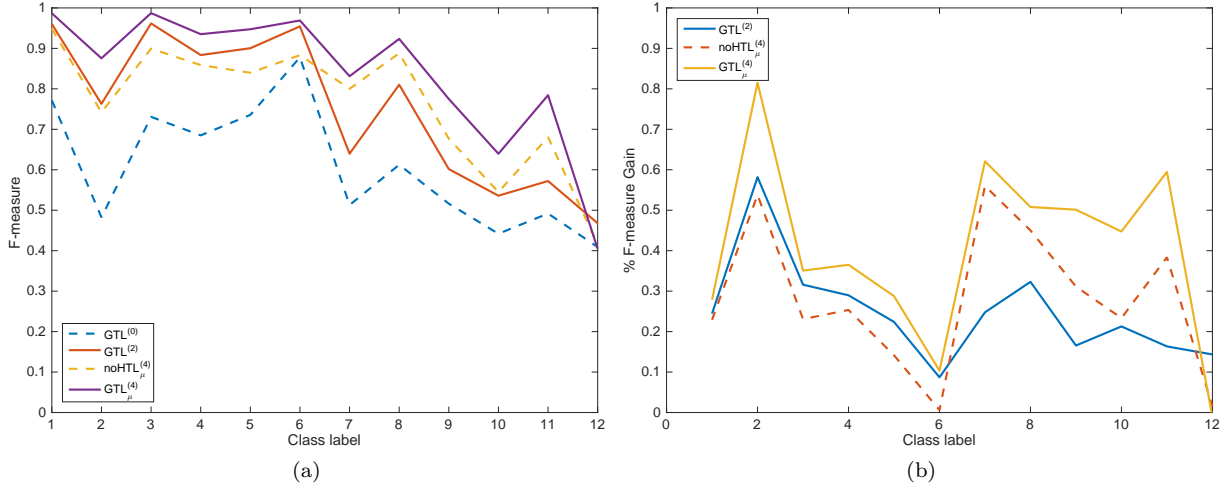


Figure 4: (a) HAPT dataset. Prediction performance per class before and after the first and the second models' exchange. (b) Prediction performance gain per class after the first and the second model exchange.

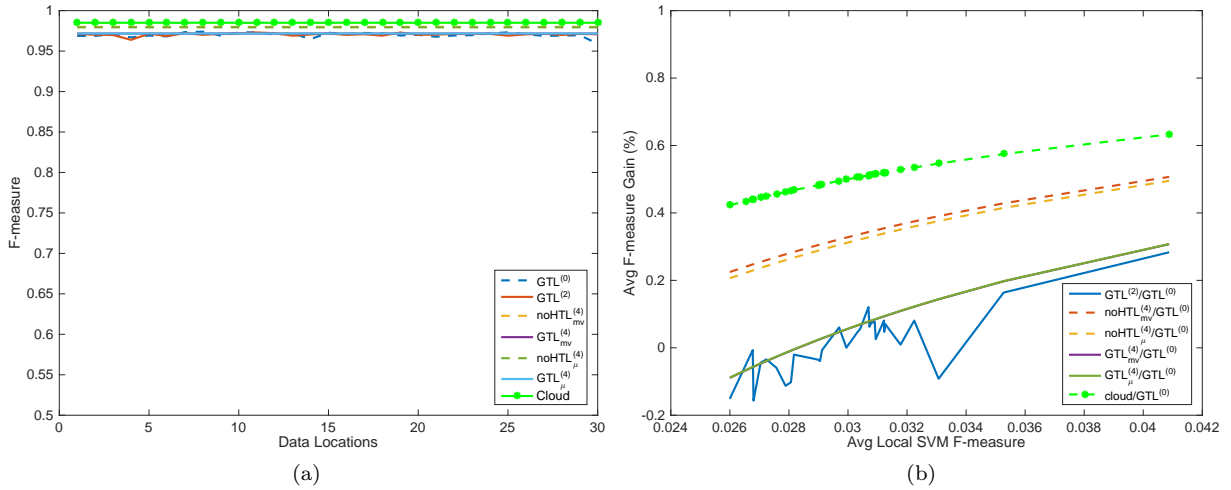


Figure 5: MNIST balanced. Prediction performance (a) and prediction performance gain (b) comparison per single location after each step of the considered distributed learning approaches for both HTL and noHTL versions.

yield an F-measure close to 1, as in the case of Cloud (but, clearly, without generating *any* traffic on the network).

6.4. Case Study III: MNIST with class unbalance

We now consider a different situation in which data is not uniformly distributed between users. Here we refer to the situation represented in Figure 2b where some classes are less represented than others. In this way we simulate a scenario where some types of information are more difficult to be sensed with respect to others.

Although the type of imbalance is the same as in the HAPT dataset, here the behaviour of GTL compared to noHTL is different. Looking at Figure 7a and 7b we see that after each step of GTL we obtain an improvement in terms of prediction performance. In this case the transfer of knowledge from one device to another allows us to obtain in Step 2 ($GTL^{(2)}$) an improvement in prediction ranging from 50% to 70%.

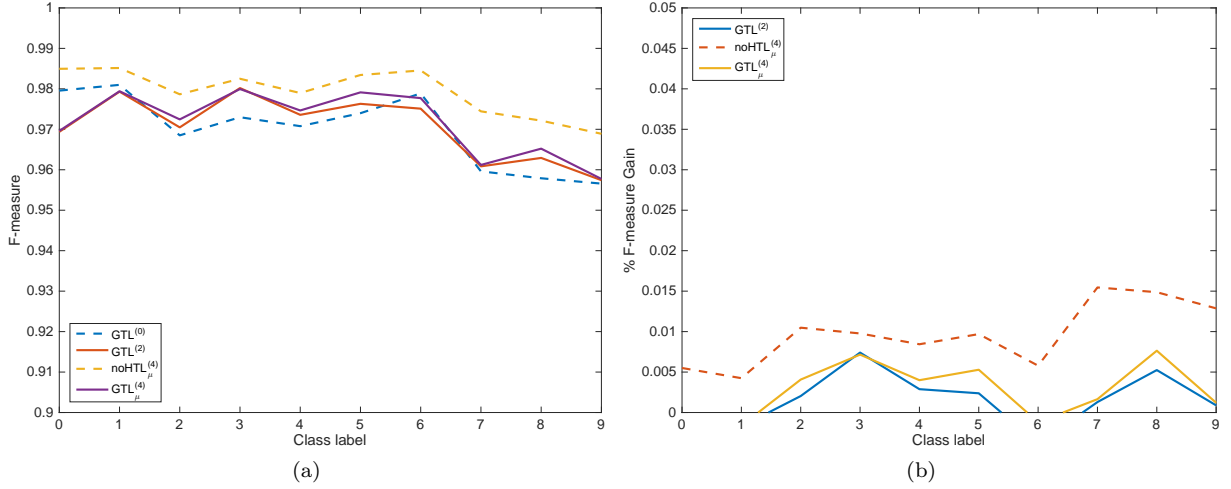


Figure 6: MNIST balanced. (a) Prediction performance per class before and after the first and the second models' exchange. (b) prediction performance gain per class after the first and the second model exchange.

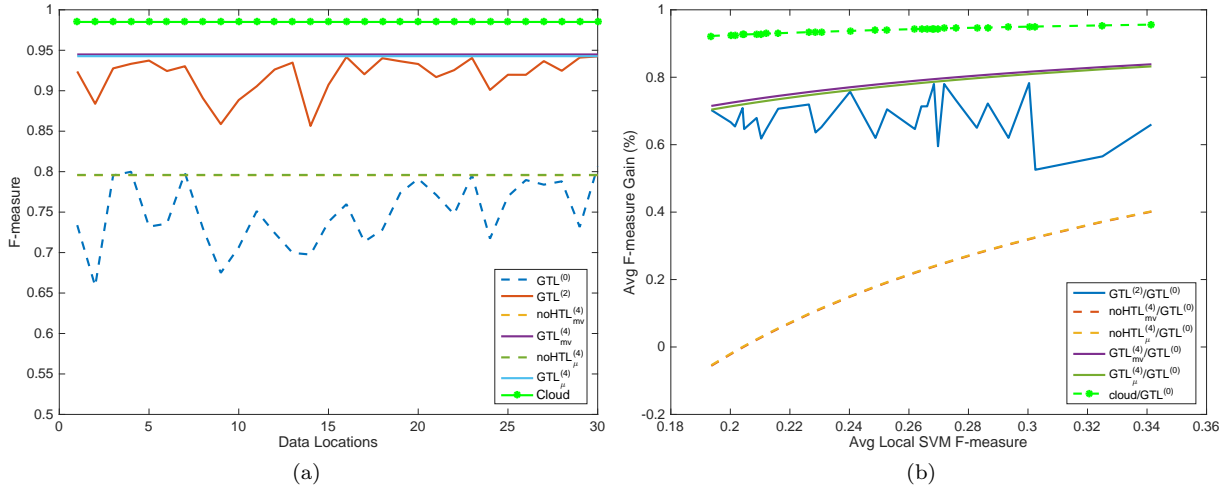


Figure 7: MNIST with class unbalance. Prediction Performance (a) and Prediction Performance Gain (b) comparison per single location after each step of the considered distributed learning approach for both GTL and noHTL versions.

Moreover, after the second phase of model aggregation in Step 4 ($GTL^{(4)}$) we obtain a further improvement in performance in which all devices obtain a final F-measure value of 0.95. If we look at the performance of the noHTL solution we notice that the combination of models is beneficial with respect to the performance of the local models, but is it not sufficient to overcome poor representation of some classes at some locations. With respect to the HAPT dataset, which was also class unbalanced, here GTL outperforms noHTL also before aggregation (i.e., after Step 2) thanks to transfer of knowledge across locations. This is due to the fact that poorly represented classes in this case are even less represented than in HAPT.

Looking at Figures 8a and 8b the benefit of GTL is even more clear. In fact if we look at the prediction performance per class and the performance gain per class we notice that, thanks to transfer of knowledge in HTL, each device is able to learn a model that, on the one hand, improves the prediction performance of quite well represented classes and, most importantly, drastically helps to fill the performance gap for those classes the are scarcely represented. The reason of this performance improvement is that the knowledge extracted

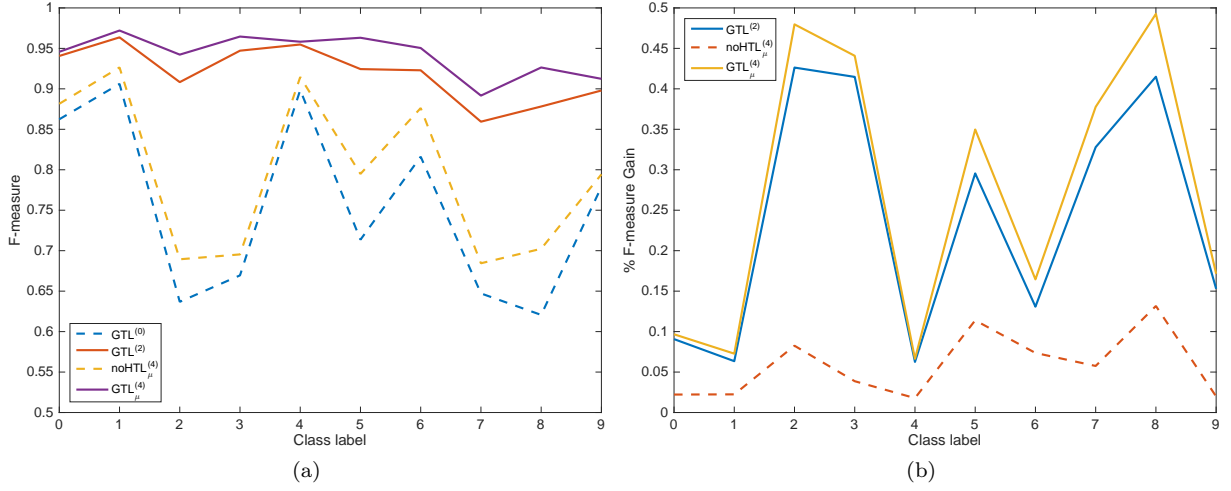


Figure 8: MNIST with class unbalance. (a) Prediction Performance per class before and after the first and the second models' exchange. (b) Prediction Performance Gain per class after the first and the second model exchange.

locally from poorly represented classes is transferred and aggregated between locations, and this overcomes the lack of data points at each individual location. In fact, as shown in Figure 8b the performance gain for classes 2,3,5,7,8 is in the range 30% – 50%. Regarding the noHTL solution, in this case simply averaging local models is not sufficient to cope with poorly represented classes. In fact, we can see some improvement for the classes less represented but it is not comparable to what obtained with the GTL solution.

6.5. Case Study IV: MNIST with node unbalance

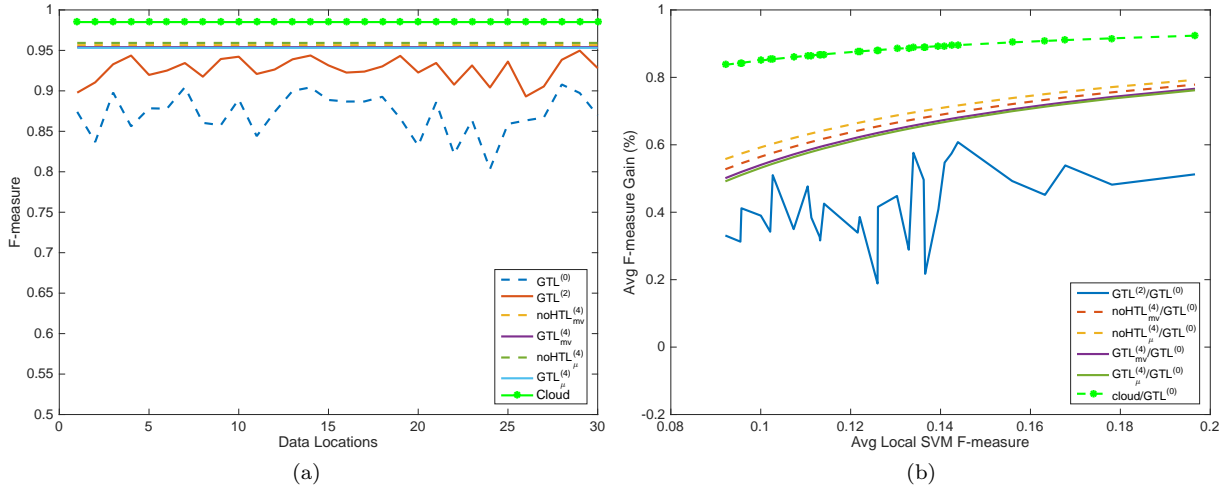


Figure 9: MNIST with node unbalance. Prediction performance (a) and Prediction Performance Gain (b) comparison per single location after each step of the proposed distributed learning approach for both HTL and noHTL versions.

Here we want to simulate a limit case where the distribution of classes collected by user devices is highly skewed. Precisely, in each local dataset 70% of data belongs to one class and the remaining 30% is equally divided between all the other classes. Since we have 30 users and 10 classes, each class is well represented in 3 different user devices and only one well represented class per user is allowed. An example of data distribution for User 1 and User 2 is shown in Figures 2c and 2d, respectively.

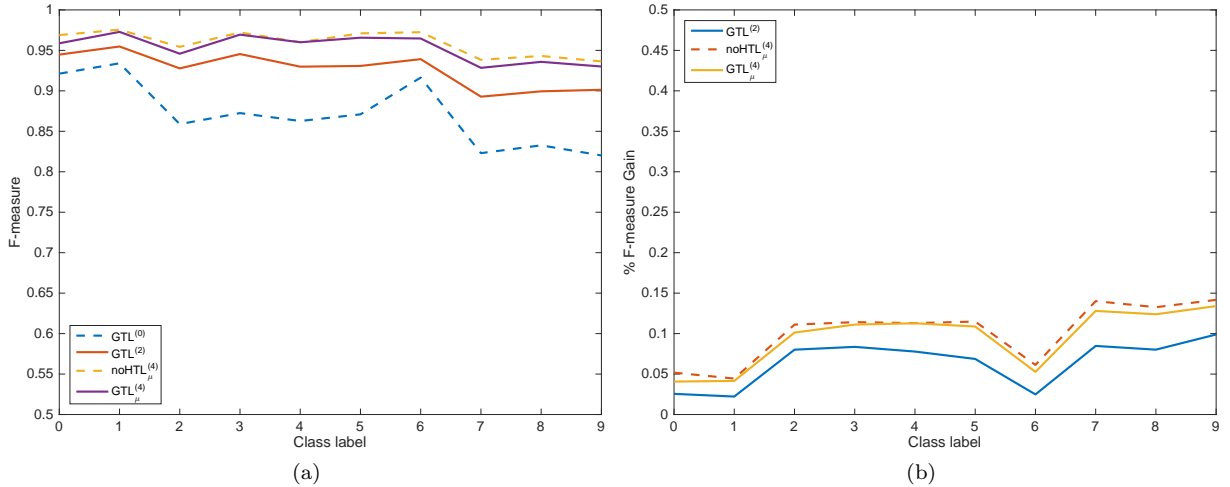


Figure 10: MNIST with node unbalance. (a) Prediction performance per class before and after the first and the second models' exchange. (b) Prediction Performance Gain per class after the first and the second model exchange.

Interestingly, as shown in Figure 9a, in this very extreme scenario we see that in terms of prediction performance, both GTL and noHTL approaches have quite similar performance. In fact they resemble the behaviour obtained in the balanced dataset, but differently from those results, the performance gain obtained by both GTL and noHTL approaches are much greater, as depicted in Figure 9b. The very same conclusion can be drawn also looking the prediction performance per class and their performance gain (Figures 10a and 10b). Also here we see that GTL and noHTL yield almost the same performance, and both drastically outperform the local models. This tells that, in case of node unbalance, distributed learning is able to “re-balance” representativeness of classes across nodes, ultimately yielding the same performance that also local model would obtain in case of completely balanced datasets.

7. Robustness to malicious behaviour

In order to further investigate the suitability of the proposed distributed learning solutions we evaluate its robustness in presence of “malicious” devices. Precisely, we consider a scenario in which s' out of s devices involved in the learning process are “malicious” and their purpose is to affect negatively the accuracy of the model learnt during the distributed learning process. In order to simulate such scenario we assume that during Step 1 of the GTL and noHTL procedures, the partial models sent by the s' devices are corrupted. In this analysis a model can be partially or totally corrupted. In order to corrupt a model, we randomly select a subset of its parameters and we replace them with random numbers generated according to a normal distribution with zero mean and unitary standard deviation. In order to identify the model's parameters to be replaced (i.e., corrupted), for each parameter p we perform a random trial according to a Bernoulli distribution with parameter p . Through the parameter p we control (on average) the percentage of corrupted model's parameters, e.g., if $p = 0.25$, 25% of the nodes (on average) will produce corrupted models. We are interested in quantifying the prediction performance degradation induced by the injection of corrupted model in the distributed learning process.

In our simulation we identify two separate scenarios, called respectively Malicious1 and Malicious2. In the Malicious1 scenario, the malicious devices send to all the other nodes a fully corrupted partial model, i.e., all the model's parameters are random values. In order to evaluate the robustness of both GTL and noHTL in presence of such type of attacks, we varied the percentage of malicious devices, i.e., 25%, 50%, 75%. Results are presented in Table 1 and 2. We notice a drastic difference in performance between GTL and noHTL for both the datasets considered. GTL proves to be more robust to the presence of malicious nodes.

The main reason is that with GTL, devices are able to i) identify and select the most informative sources (i.e. the partial models with a real informative content) and, most importantly, ii) exclude automatically partial models that do not contain useful knowledge. Clearly, when the number of malicious devices (and models) increases too much, the performance of GTL slightly decreases but it still remains very good. Conversely, as we may expect, the performance of noHTL is strongly affected by the presence of “malicious” partial models. In fact, the noHTL procedure averages the partial models in order to come up with a final model, thus when the number of malicious models outnumbers the “good” ones, its performance degrades accordingly.

Table 1: MNIST balanced. F-Measure of GTL and noHTL in the Malicious1 scenario.

% Malicious devices	noHTL $_{\mu}$	GTL $_{\mu}$
25%	0.94	0.970
50%	0.72	0.972
75%	0.40	0.971

Table 2: HAPT balanced. F-Measure of GTL and noHTL in the Malicious1 scenario.

% Malicious devices	noHTL $_{\mu}$	GTL $_{\mu}$
25%	0.83	0.970
50%	0.56	0.95
75%	0.24	0.95

In the Malicious2 scenario we consider the case in which all the devices are malicious but the partial models they exchange with each other during Step 1 are only partially corrupted. Specifically we evaluate both GTL and noHTL varying the corruption level of exchanged models. In our simulations, the percentage of corrupted parameters at each node is 25%, 50%, 75%. Note that this case also represents non-malicious scenarios, where for any other reasons the partial models parameters are inaccurate or corrupted. Results are reported in Tables 3 and 4. Similarly to the Malicious1 scenario, we see that GTL is able to select which parameters are informative and which are not, thus preserving an overall good prediction performance. Regarding noHTL we see also in this case that the presence of corrupted parameters strongly affects its prediction performance.

Table 3: MNIST balanced. F-Measure of GTL and noHTL in the Malicious2 scenario.

% of corrupted params.	noHTL $_{\mu}$	GTL $_{\mu}$
25%	0.90	0.97
50%	0.77	0.97
75%	0.43	0.96

Table 4: HAPT balanced. F-Measure of GTL and noHTL in the Malicious2 scenario.

% of corrupted params.	noHTL $_{\mu}$	GTL $_{\mu}$
25%	0.78	0.960
50%	0.43	0.96
75%	0.29	0.96

8. Network overhead performance

We hereafter focus on the analysis of the network traffic generated by the different learning schemes considered in the paper. With network overhead (OH) we refer to the amount of information that must be sent between all the data locations in order to accomplish the learning task. We recall that in the GTL

solution, local information is sent over the network twice, i.e. to send the GTL⁽⁰⁾ models and to send the GTL⁽²⁾ models after Step 2. Therefore, the amount of information sent in GTL is given by the size of the coefficients of the model in the two steps. This is $\omega^{(0)}$ and $\omega^{(1)}$, respectively. Specifically, $\omega^{(0)}$ is a vector of d coefficients where d is the dimensionality of the data points $\mathbf{x} \in \mathbf{X}$. On the other hand, it holds that $\omega^{(1)} \in \mathbb{R}^{d+s-1}$, where s is the number of data locations. Table 5 reports the relevant notation.

Table 5: Network overhead notation

s	n. of data locations
k	n. of classes
N	n. of data points in the entire dataset
$\omega^{(0)} \in \mathbb{R}^d$	coefficients of the SVM model
$\omega^{(1)} \in \mathbb{R}^{d+s-1}$	coefficients of the GTL model
$d^{(0)}$	n. of non-null coefficients in $\omega^{(0)}$
$d^{(1)}$	n. of non-null coefficients in $\omega^{(1)}$

The network overhead generated by GTL is computed as follows:

$$OH^{GTL} = OH^{(0)} + OH^{(1)} \quad (7)$$

where

$$OH^{(0)} = s(s-1)d^{(0)}k \quad (8)$$

$$OH^{(1)} = s(s-1)d^{(1)}k \quad (9)$$

With respect to $OH^{(0)}$, the expression comes from the fact that after step 1 each location has to send to the other $s-1$ locations a classifier for each class. As each classifier consists in $d^{(0)}$ *non-null* coefficients, and we have k classes, the formula is straightforward. With respect to $OH^{(1)}$, in step 3 each location has to send again a classifier per class, but this time the classifier consists in $d^{(1)}$ *non-null* coefficients.

Table 6 reports the network overhead for each models' exchange phase of the GTL procedure. As we can see, the most expensive phase is the exchange of the local models. The second one, instead, has a negligible cost if compared to the first one. The main reason is the fact that the number of non-null coefficients after the first GTL step (i.e., Step 2 in the algorithm) is typically much smaller than the number of non-null coefficients of the local models. This is a general property of GreedyTL, that also works as a feature selection algorithm [23]. Remember that in our dataset data points are not raw data, but are features extracted locally from the raw data. In most IoT applications, instead, knowledge extraction would be done starting from the raw data, which will significantly impact the overhead of the Cloud solution. Specifically, the table also presents the overhead of the Cloud solution, in both cases where features (OH^{cl}) or raw data (OH^{raw}) are collected. These results clearly indicate that using GTL as opposed to a centralised cloud solution achieves a drastic reduction in terms of network overhead, which amounts to 52% and 83% in the case of the HAPT and MNIST datasets, respectively. Note that if we consider the raw data instead of pre-processed data (as it would be common for many applications) the reduction in overhead would jump to 77% and 83% for HAPT and MNIST datasets, respectively. This is an extremely good result, if one considers the obtained prediction performance.

Table 6: Empirical network overhead for the GTL solution

	$OH^{(0)}$	$OH^{(1)}$	OH^{tot}	OH^{cl}	OH^{raw}	Gain	Gain _{raw}
HAPT	20MB	3MB	23MB	48MB	103MB	52%	77%
MNIST	21MB	4MB	25MB	148MB	358MB	83%	93%

Let us now consider the network overhead performance of the noHTL solution. The network overhead triggered by the noHTL distributed learning procedure depends on the models' aggregation method. In fact, if we want to compute the mean model (Consensus-based aggregation), it is sufficient to collect all models $\omega^{(0)}$ into one device, compute the mean model and send it back to all the other devices. Conversely, if we

consider to use a majority voting approach, all the devices must have all the $\omega^{(0)}$ models. The network overhead generated by noHTL is computed as follows:

$$OH_{\mu}^{noHTL} = 2k(s-1)d^{(0)} \quad (10)$$

$$OH_{mv}^{noHTL} = ks(s-1)d^{(0)} \quad (11)$$

where $\bar{d}^{(0)}$ is the size of the mean model sent back to all devices. It is clear that Consensus-based aggregation is more efficient, as it cuts traffic by a factor equal to the number of locations, s .

Table 7 shows the performance of both versions of noHTL. It is confirmed that using Consensus-based aggregation is way more efficient (one order of magnitude) than Majority voting. As, in terms of prediction performance, there is no significant difference between the two, typically the former would be preferred. Also note that, as expected, the overhead of noHTL with Majority voting is comparable with that of GTL.

Therefore, we can conclude that (i) both GTL and noHTL provide a drastic reduction of overhead with respect to Cloud-based solution, also when data are pre-processed locally to extract features; (ii) GTL generates more traffic in the network with respect to noHTL with Consensus-based aggregation, but there are cases where it can provide a very significant gain in terms of prediction performance. The choice between GTL and noHTL depends thus on the specific requirements in terms of predictivity vs. network traffic trade-off. We come back on this point in Section 9, where we show how to significantly reduce the GTL overhead without affecting its prediction performance.

Table 7: Empirical network overhead for noHTL solution.

	OH_{μ}^{noHTL}	OH_{mv}^{noHTL}	$OH^{cl.}$	OH^{raw}	Gain $_{\mu}$	Gain $_{\mu}^{raw}$	Gain $_{mv}$	Gain $_{mv}^{raw}$
HAPT	2MB	20MB	48MB	103MB	96%	98%	58%	81%
MNIST	1.45MB	21MB	148MB	358MB	99%	99.5%	86%	94%

8.1. Bound on GTL network overhead

In order to deeply understand the behaviour of the GTL solution from the point of view of the network overhead, we derived, under some reasonable assumption, an upper bound of the network overhead. Our only assumption is that the model learnt by GreedyTL at Step 2 has less non-zero elements than the base model. Formally, provided that

$$d^{(1)} \leq d^{(0)}$$

and assuming, as it is typically the case, that the number of non-null coefficients of the learners ($d^{(0)}$ and $d^{(1)}$) is much higher than the number of locations s , the network overhead is upper bounded as follows:

$$OH^{tot} \leq OH^{up} \triangleq 2ks^2d^{(0)}. \quad (12)$$

To obtain Equation 12 we note that in general we can approximate $OH^{(0)}$ as $s^2d^{(0)}k$. Under the assumption $d^{(1)} \gg s$, $OH^{(1)}$ can be approximated as $s^2d^{(1)}k$, and because $d^{(1)} \leq d^{(0)}$, $OH^{(1)} \leq OH^{(0)}$ holds true. Therefore, the following also holds:

$$\begin{aligned} OH^{(0)} + OH^{(1)} &\leq 2 * OH^{(0)} \\ &\leq 2k(s(s-1)d^{(0)}) \\ &\leq 2ks^2d^{(0)} - 2ksd^{(0)} \\ &< 2ks^2d^{(0)} \end{aligned} \quad (13)$$

Note that the bound in Equation 12 can be quite pessimistic. In many cases (as with our dataset), actually $d^{(1)} \ll d^{(0)}$ holds, and therefore OH^{tot} can be well approximated with $OH^{(0)} \simeq s^2kd^{(0)}$. However, in the following we use the more exact (but pessimistic) bound given by Equation 12, thus presenting worst-case results for the network overhead with GTL.

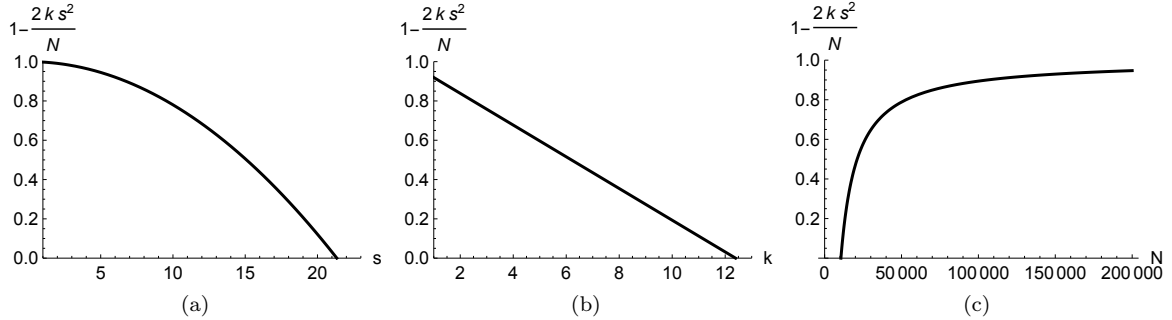


Figure 11: Parameters' sensitivity analysis of the network gain with GTL.

We can exploit Equation 12 to derive a lower bound on the network gain. Specifically, considering that in the case of a centralised cloud based system the overhead is $OH^{cloud} = Nd^{(c)}$ where $d^{(c)}$ is the dimensionality of each data point, we can define a lower bound on the gain as follows

$$\underline{G} = 1 - \frac{OH^{up}}{OH^{cloud}} = 1 - \frac{2ks^2d^{(0)}}{Nd^{(c)}}. \quad (14)$$

We use \underline{G} to perform a sensitivity analysis of the network gain with GTL. Note that in the following we assume, as it is the case of our datasets, that the dimensionality of the original data points is approximately the same of the dimensionality of the $GTL^{(0)}$ coefficients (note that in our dataset the dimensionality of raw data would be even larger, thus our analysis provides an even lower bound on the possible gain of GTL), and thus $\underline{G} \simeq 1 - \frac{2ks^2}{N}$ holds. Precisely in order to study the impact of each parameter, for each graph in the following we keep two parameters fixed (we use the values obtained by simulations) and we vary the remaining one. From Fig. 11b we see that the gain is linear with the number of classes k . This is quite obvious because keeping fixed the size of the dataset and the number of data locations, more classes means more binary models to be sent over the network. Figure 11c is more interesting, as it shows that the more the size of the dataset (N) increases, the more it becomes advantageous to use GTL, as the relative cost of exchanging models instead of data becomes negligible. This is also the case we have observed in simulation, reported in Table 6: the MNIST dataset is larger than HAPT, and this results in a higher gain in using GTL. Also note that the curve is concave, and thus also for relatively small data sizes (with respect to the number of locations and dimensionality of our dataset) the cost of GTL becomes already almost negligible.

Conversely, looking at Figure 11a, we see that there is a limit on the number of data locations, above which the exchange of model coefficients becomes too expensive. Let us define as μ_D the average number of data points per location, such that $N = s\mu_D$. The gain can then be written as follows:

$$\underline{G} = 1 - \frac{2ks^2d^{(0)}}{Nd^{(c)}} \sim 1 - \frac{2ks^2}{s\mu_D} = 1 - \frac{2ks}{\mu_D} \quad (15)$$

This form of \underline{G} has an intuitive explanation. For each location, ks is the network overhead of using GTL, as it is the total size of models' parameters to be sent. On the other hand, μ_D is the per-site cost of a cloud-based solution. As soon as the number of locations increases above $\frac{\mu_D}{2k}$ using GTL becomes not advantageous anymore.

9. Tuning the prediction vs. network overhead trade-off

From the results presented in Section 8 it becomes clear that both GTL and noHTL have pros and cons. In general noHTL $_{\mu}$ is the best choice in terms of network overhead, however it is not always the best solution in terms of prediction performance. As shown before, it is highly dependent on the distribution of classes between different locations. Moreover, from the network overhead point of view, the GTL and

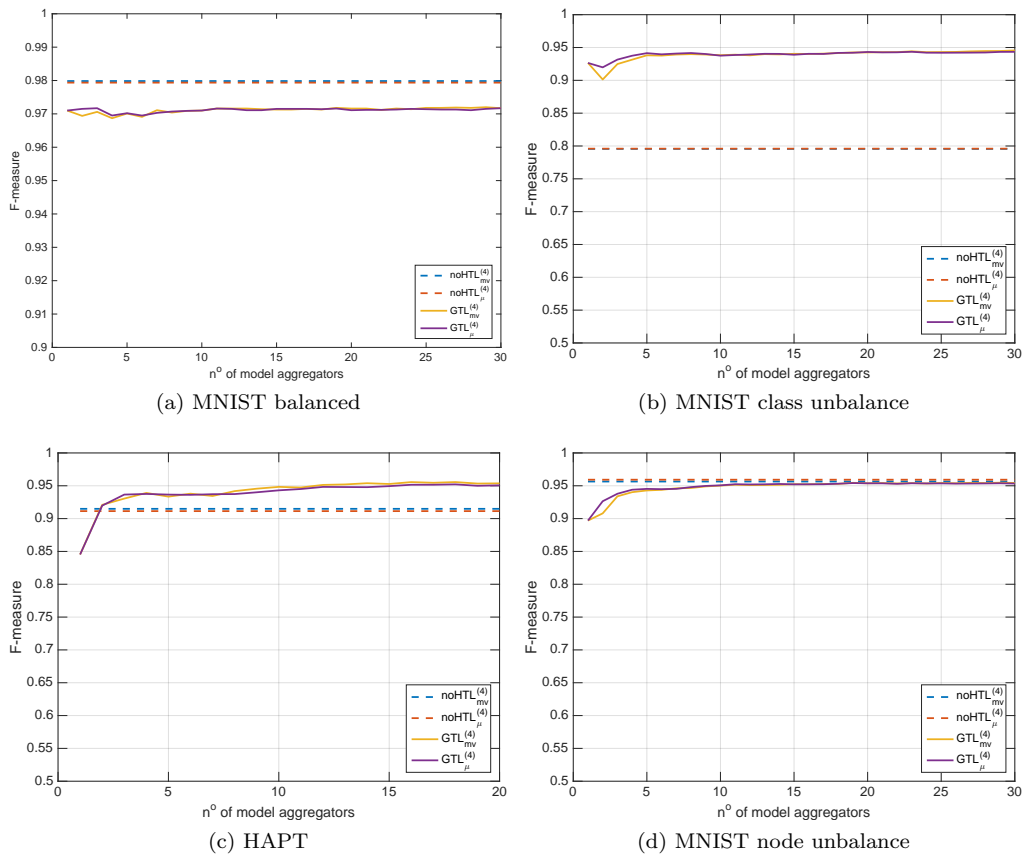


Figure 12: Prediction performance increasing the number of aggregators involved in the distributed learning process for both GTL and noHTL.

noHTL $_{\mu}$ approaches represent the upper and lower limits of the traffic that we can generate with such type of distributed learning system. One interesting question is if there exist an intermediate solution in terms of models exchange that limits the traffic generated but leaves the prediction performance unaffected.

In order to shed some light on this point, for all the scenarios presented before we performed a sensitivity analysis adopting the following approach. Regarding GTL, instead of performing the models' synchronisation in parallel for all devices, we do it for one device at a time in an incremental fashion. We pick a certain number of nodes as *model aggregators*. This number can vary between 1 and the total number of nodes. All nodes compute their local models as per original Step 0. We then send the local models only to the aggregators, which perform Step 2 of the algorithm, thus computing an aggregate model based on the ones received, using the local dataset for training. Finally, only the aggregators perform Steps 3 and 4, i.e., they exchange and aggregate the models they have computed in Step 2. The final model is sent back to all nodes. In terms of overhead, when the number of aggregators is equal to 1, this is equivalent to noHTL with Consensus-based aggregation. When we use all nodes as aggregators, this is equivalent to the original GTL algorithm.

In Figure 12 we show to what extent the performance of GTL depends on the number of aggregators involved in the procedure, for each different experimental setup we presented before. For comparison, we also report the performance of noHTL, which clearly does not depend on the number of GTL aggregators. More precisely, it would be possible to define a scheme for noHTL $_{mv}$ by exchanging only a limited number of models. We have decided to show here the performance of the original noHTL $_{mv}$ scheme, as a worst-case comparison for GTL. For the case where the dataset is balanced (Figure 12(a)), there is no significant gain in using additional model aggregators. More interesting is the case of unbalanced datasets. In all cases GTL benefits from an additional number of aggregators. However, it is very interesting to note that only a small number of aggregators is sufficient to already obtain the prediction performance of GTL with complete exchange of models across all locations. Therefore, it is possible to appropriately tune GTL to outperform noHTL in terms of prediction performance, while approximating very closely the performance of noHTL $_{\mu}$ in terms of network overhead.

10. Dynamic scenario

In order to complete the analysis of the distributed learning approaches considered in this paper, in this section we evaluate their applicability to a more dynamic scenario in which devices contributing to the distributed learning process are not necessarily all present at the same time, but they may appear (and disappear) at different time instants. This configuration represents, for example, mobile social networking applications where users participate only when they are in a specific physical location (e.g., a gym, a park, a museum), and only for the time they spend there. Therefore, in this case the learning phase is intended as a continuous process contributed by every device entering the location. Note that in this case, in order to allow the continuous learning process, we need to assume that in the location there exist a permanent device (e.g. a totem) able to communicate with all the other devices, whose purpose is to store (and provide) to newly entered devices the information regarding the state of learning process executed so far. Or, it would be possible to use solutions like Floating Content [43] in order to make the model available in the physical area by using only mobile nodes that move inside it.

In this dynamic scenario the learning process is done as follows. When a number s of devices enter into the location, they receive the aggregate model m that has been previously built by other devices (not necessarily still present) that executed the GTL learning procedure. The s devices normally execute the GTL procedure, including in the distributed learning phase also the aggregate model m . Once the learning phase is finished and a new aggregate model m' is obtained, the latter is combined with the previous version of the model using the exponential moving average:

$$m_{new} = \alpha m_{old} + (1 - \alpha)m' \quad (16)$$

where $0 < \alpha \leq 1$ is a smoothing parameter used to balance the combination of the old model with the new one. Note that, in this settings we assume that a single learning phase is atomic, i.e., during the learning phase devices involved in it do not change and no new devices can join.

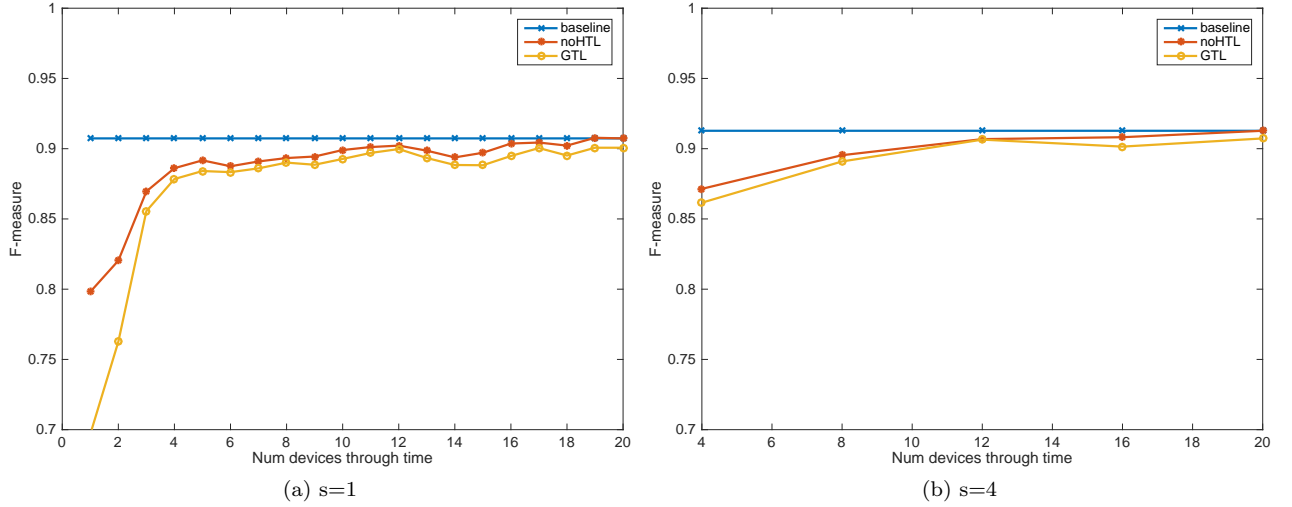


Figure 13: Dynamic scenario. HAPT dataset. Prediction performance evolution with 1 and 4 new coming devices for each learning phase, respectively.

We are interested in measuring i) the evolution of prediction performance of both GTL and noHTL as long as devices arrive in the location to contribute to the continuous learning process and ii) the amount of traffic generated. Regarding the generated traffic, assuming that a permanent device, say G , exists that stores the models, we point out that in addition to the traffic related to each learning phase we have to include the traffic connected to sending the model m to the s devices at the beginning of the learning procedure, and the one for sending the m' model to the permanent device. Formally, the additional traffic generated by the communication between G and the s devices is

$$OH^G = d^{(0)}k(s+1) \quad (17)$$

therefore in this scenario the total network overhead for GTL is

$$OH^{dynGTL} = OH^{GTL} + OH^G \quad (18)$$

Conversely, for noHTL the way to compute the network overhead remains unchanged because the s devices do not have to perform a retraining on their local data exploiting additional information contained in the aggregate model. In fact, their models are sent to the devices holding the aggregate model m which computes the updated one (m') and send it back to the s devices.

Let us now present the performance of both GTL and noHTL in this dynamic scenario. Simulations are performed using both HAPT and MNIST datasets with balanced class distribution. In our simulations the number of devices entering the location at each new arrival is constant. For the sake of comparison we used as baseline the prediction performance obtained by noHTL in Sections 6.2 and 6.3. In Figures 13 and 14 we show the prediction performance of both GTL and noHTL. As we can see, in both scenarios both approaches are able to converge after some time to the performance we would obtain running the same algorithms in presence of all device at the same time (see the baseline curve). Another interesting fact is that both GTL and noHTL, apart from the initial learning phases, converge to the same performance. This suggests that in this specific case, using a learning mechanism based on Hypothesis Transfer Learning does not provide any significant advantage. We think that this could be due to the fact that the number of devices involved in each separate learning phase is so small that all the model they provide are useful to build the aggregate model and as a consequence none of them can be discarded.

From the network overhead point of view, both approaches prove to be beneficial w.r.t. a cloud solution. Note that in this case the network overhead is computed averaging the traffic generated during each learning

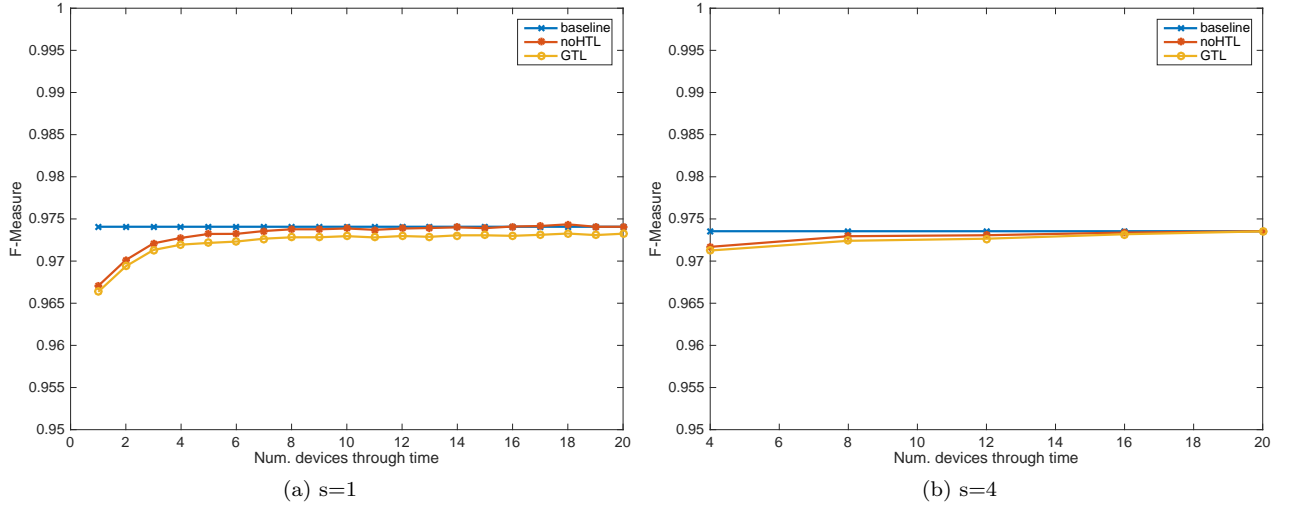


Figure 14: Dynamic scenario. MNIST dataset. Prediction performance evolution with 1 and 4 new coming devices for each learning phase, respectively.

Table 8: HAPT Dataset. Network overhead for different values of s .

	s	OH^{noHTL}	OH^{dynGTL}	Gain noHTL	Gain dynGTL
HAPT	1	0.1 MB	0.1MB	94%	94%
HAPT	4	0.4 MB	1MB	94%	84%

phase. The percentage gains are computed with respect to the amount of data held by devices involved in it (i.e., the amount of data that would be transferred in a Cloud-based approach). Looking at Tables 8 and 9, which report the average network overhead computed after each learning phase, we see that for both datasets, GTL and noHTL save more than 95% of traffic. This results are in line with the ones presented in Section 8 and confirm the efficiency of distributed learning, also in dynamic scenarios.

11. Conclusions

In this paper we study the performance of distributed learning solutions for Fog Computing environments. Precisely, we are interested in comparing the ability of the different distributed learning approaches to accomplish a general machine learning task (such as pattern recognition) on a dataset that is spread over several and separated physical locations, without moving the data from where it is generated.

We have defined two types of algorithms, GTL and noHTL, respectively. The first one is based on the Hypothesis Transfer Learning framework. Nodes compute partial models based on local data, and then exchange all models between each other. They re-compute another model that combines all the ones received, exchange again the new models and aggregate them by averaging the models coefficient. On the other hand, noHTL is a simpler scheme where nodes compute the local models, exchange them, and aggregate them either through a standard consensus-based mechanism (i.e., again computing the average coefficients of the received models), or based on a majority voting scheme.

Table 9: MNIST Dataset. Network overhead for different values of s .

	s	OH^{noHTL}	OH^{dynGTL}	Gain noHTL	Gain dynGTL
MNIST	1	0.05 MB	0.05MB	98%	98%
MNIST	4	0.2 MB	1MB	98%	95%

We have analysed in detail the performance of these two algorithms both in terms of prediction performance and in terms of network overhead. We have used two reference datasets in the machine learning literature, i.e. the HAPT and MNIST datasets. In all cases we have compared the performance of the distributed learning solutions with those of a cloud-based solution where all data have to be sent to a central cloud platform. We have considered both balanced cases, i.e. where all nodes “see” the same distribution of data points and all classes of data are equally represented, as well as unbalanced cases, where either classes are unbalanced, or nodes see very different distributions of data points. Our results show that adopting such kind of distributed learning approaches we obtain prediction performance comparable with a cloud-based solution, while saving between 60% and 90% of the network traffic. Among the two considered distributed solutions, GTL in several cases yields better prediction performance, at the cost of higher traffic overhead. However, we have also defined and evaluated a GTL solution where traffic can be made almost equivalent to noHTL, without impacting on prediction performance.

Summarising, we think the results presented in this paper are very encouraging. They show that it is possible to analyse large-scale datasets collected by a large number of mobile devices, without necessarily transferring all these data to some central cloud platform, but through local analysis and appropriate distributed learning schemes. This is important, because the proposed solutions can drastically cut network traffic thus contributing to avoid congestion on wireless access networks. In addition, our algorithms lend themselves to cases where data needs to stay where it is collected for privacy and ownership reasons, but knowledge can be extracted from it nevertheless.

Acknowledgment

This work is partly funded by the European Commission under the H2020 REPLICATE (691735) , SoBigData (654024), and AUTOWARE (723909) projects.

References

References

- [1] A. S. Vincentelli, Let’s get physical: Adding physical dimensions to cyber systems, in: Low Power Electronics and Design (ISLPED), 2015 IEEE/ACM International Symposium on, 2015, pp. 1–2. doi:10.1109/ISLPED.2015.7273478.
- [2] Cisco. Cisco visual networking index: Global mobile data traffic forecast update, 2015–2020 [online] (2016).
- [3] M. Conti, S. K. Das, C. Bisdikian, M. Kumar, L. M. Ni, A. Passarella, G. Roussos, G. Tröster, G. Tsudik, F. Zambonelli, Looking ahead in pervasive computing: Challenges and opportunities in the era of cyber–physical convergence, *Pervasive and Mobile Computing* 8 (1) (2012) 2 – 21.
- [4] E. Borgia, The internet of things vision: Key features, applications and open issues, *Computer Communications* 54 (2014) 1 – 31. doi:http://dx.doi.org/10.1016/j.comcom.2014.09.008.
URL <http://www.sciencedirect.com/science/article/pii/S0140366414003168>
- [5] E. Cavalcante, J. Pereira, M. P. Alves, P. Maia, R. Moura, T. Batista, F. C. Delicato, P. F. Pires, On the interplay of internet of things and cloud computing: A systematic mapping study, *Computer Communications* 89–90 (2016) 17 – 33, internet of Things Research challenges and Solutions. doi:http://doi.org/10.1016/j.comcom.2016.03.012.
URL <http://www.sciencedirect.com/science/article/pii/S0140366416300706>
- [6] E. Borgia, D. G. Gomes, B. Lagesse, R. Lea, D. Puccinelli, Special issue on “internet of things: Research challenges and solutions”, *Computer Communications* 89–90 (2016) 1 – 4, internet of Things Research challenges and Solutions. doi:http://doi.org/10.1016/j.comcom.2016.04.024.
URL <http://www.sciencedirect.com/science/article/pii/S0140366416301797>
- [7] ETSI TC M2M. ETSI TS 102 690 v2.1.1 (2013-10) – Machine-to-Machine Communications (M2M); Functional Architecture, 2013 [online].
- [8] F. Rebecchi, M. Dias de Amorim, V. Conan, A. Passarella, R. Bruno, M. Conti, Data offloading techniques in cellular networks: A survey, *Communications Surveys Tutorials, IEEE PP* (99) (2014) 1–1. doi:10.1109/COMST.2014.2369742.
- [9] L. Valerio, R. Bruno, A. Passarella, Cellular traffic offloading via opportunistic networking with reinforcement learning, *Computer Communications* 71 (2015) 129 – 141. doi:http://doi.org/10.1016/j.comcom.2015.09.004.
URL <http://www.sciencedirect.com/science/article/pii/S0140366415003242>
- [10] F. Rebecchi, L. Valerio, R. Bruno, V. Conan, M. D. de Amorim, A. Passarella, A joint multicast/d2d learning-based approach to {LTE} traffic offloading, *Computer Communications* 72 (2015) 26 – 37. doi:http://doi.org/10.1016/j.comcom.2015.09.025.
URL <http://www.sciencedirect.com/science/article/pii/S0140366415003679>
- [11] NYTimes, Customers angered as iphones overload at&t, new york times.

- [12] J. Estrada-Jimanez, J. Parra-Arnau, A. Rodriguez-Hoyos, J. Forné, Online advertising: Analysis of privacy threats and protection approaches, *Computer Communications* 100 (2017) 32 – 51. doi:<http://doi.org/10.1016/j.comcom.2016.12.016>.
URL <http://www.sciencedirect.com/science/article/pii/S0140366416307083>
- [13] G. P. Association. 5g and the factories of the future [online] (2015).
- [14] P. G. Lopez, A. Montresor, D. Epema, A. Datta, T. Higashino, A. Iamnitchi, M. Barcellos, P. Felber, E. Riviere, Edge-centric computing: Vision and challenges, *ACM Sigcomm Computer Communication Review* (2015).
- [15] F. Bonomi, R. Milito, J. Zhu, S. Addepalli, Fog computing and its role in the internet of things, in: *Proceedings of the First Edition of the MCC Workshop on Mobile Cloud Computing, MCC '12*, ACM, New York, NY, USA, 2012, pp. 13–16. doi:10.1145/2342509.2342513.
URL <http://doi.acm.org/10.1145/2342509.2342513>
- [16] M. Conti, S. Giordano, M. May, A. Passarella, From opportunistic networks to opportunistic computing, *Comm. Mag.* 48 (9) (2010) 126–139. doi:10.1109/MCOM.2010.5560597.
URL <http://dx.doi.org/10.1109/MCOM.2010.5560597>
- [17] B. McMahan, D. Ramage, Federated learning: Collaborative machine learning without centralized training data (2017).
URL <https://research.googleblog.com/2017/04/federated-learning-collaborative.html?m=1>
- [18] H. Kagermann, W. Wahlster, J. Helbig, Recommendations for implementing the strategic initiative industrie 4.0, *Tech. rep.*, German National Academy of Science and Engineering (2013).
- [19] A. S. Teles, F. J. da Silva e Silva, M. Endler, Situation-based privacy autonomous management for mobile social networks, *Computer Communications* 107 (2017) 75 – 92. doi:<http://doi.org/10.1016/j.comcom.2017.04.003>.
URL <http://www.sciencedirect.com/science/article/pii/S0140366417303961>
- [20] T. Kärkkäinen, P. Houghton, L. Valerio, A. Passarella, J. Ott, Demo: Here&now - data-centric local social interactions through opportunistic networks, in: *11th ACM MobiCom Workshop on Challenged Networks*, New York, USA, 2016.
- [21] K. Thilakarathna, F.-Z. Jiang, S. Mrabet, M. A. Kaafar, A. Seneviratne, G. Xie, Crowd-cache: Leveraging on spatio-temporal correlation in content popularity for mobile networking in proximity, *Computer Communications* 100 (2017) 104 – 117. doi:<http://doi.org/10.1016/j.comcom.2017.01.006>.
URL <http://www.sciencedirect.com/science/article/pii/S0140366417300488>
- [22] L. Valerio, A. Passarella, M. Conti, Hypothesis transfer learning for efficient data computing in smart cities environments, in: *International Conference on Smart computing (SMARTCOMP 2016)*, St. Louis, Missouri, 2016.
- [23] I. Kuzborskij, F. Orabona, B. Caputo, Transfer learning through greedy subset selection, in: *Proceedings of Intl. Conf. on Image Analysis and Processing*, 2015.
- [24] L. Breiman, Bagging predictors, *Machine Learning* 24 (2) 123–140. doi:10.1007/BF00058655.
URL <http://dx.doi.org/10.1007/BF00058655>
- [25] Y. Freund, R. E. Schapire, A decision-theoretic generalization of on-line learning and an application to boosting, *Journal of Computer and System Sciences* 55 (1) (1997) 119 – 139. doi:<http://dx.doi.org/10.1006/jcss.1997.1504>.
URL <http://www.sciencedirect.com/science/article/pii/S002200009791504X>
- [26] Y. Freund, R. E. Schapire, Y. Singer, M. K. Warmuth, Using and combining predictors that specialize, in: *Proceedings of the Twenty-ninth Annual ACM Symposium on Theory of Computing, STOC '97*, ACM, New York, NY, USA, 1997, pp. 334–343. doi:10.1145/258533.258616.
URL <http://doi.acm.org/10.1145/258533.258616>
- [27] R. A. Jacobs, M. I. Jordan, S. J. Nowlan, G. E. Hinton, Adaptive mixtures of local experts, *Neural Computation* 3 (1) (1991) 79–87.
- [28] A. Bordes, S. Ertekin, J. Weston, L. Bottou, Fast kernel classifiers with online and active learning, *J. Mach. Learn. Res.* 6 (2005) 1579–1619.
URL <http://dl.acm.org/citation.cfm?id=1046920.1194898>
- [29] J. Dean, G. Corrado, R. Monga, K. Chen, M. Devin, M. Mao, A. Senior, P. Tucker, K. Yang, Q. V. Le, et al., Large scale distributed deep networks, in: *Advances in Neural Information Processing Systems*, 2012, pp. 1223–1231.
- [30] A. Coates, B. Huval, T. Wang, D. Wu, B. Catanzaro, A. Ng, Deep learning with cots hpc systems, *JLMR* 28 (3) (2013) 1337–1345.
- [31] A. Navia-Vázquez, E. Parrado-Hernandez, Distributed support vector machines, *Neural Networks, IEEE Transactions on* 17 (4) (2006) 1091–1097.
- [32] L. Georgopoulos, M. Hasler, Distributed machine learning in networks by consensus, *Neurocomputing* 124 (2014) 2 – 12. doi:<http://dx.doi.org/10.1016/j.neucom.2012.12.055>.
URL <http://www.sciencedirect.com/science/article/pii/S0925231213003639>
- [33] S. Scardapane, D. Wang, M. Panella, A. Uncini, Distributed learning for random vector functional-link networks, *Information Sciences* 301 (2015) 271 – 284. doi:<http://dx.doi.org/10.1016/j.ins.2015.01.007>.
URL <http://www.sciencedirect.com/science/article/pii/S0020025515000298>
- [34] D. H. Wolpert, Stacked generalization, *Neural Networks* 5 (2) (1992) 241–259.
- [35] L. Valerio, A. Passarella, M. Conti, E. Pagani, Scalable data dissemination in opportunistic networks through cognitive methods, *Pervasive and Mobile Computing* 16, Part A (2015) 115 – 135. doi:<http://dx.doi.org/10.1016/j.pmcj.2014.05.005>.
URL <http://www.sciencedirect.com/science/article/pii/S1574119214000819>
- [36] A. Ng, Feature selection, l1 vs. l2 regularization, and rotational invariance, in: *Intl Conference on Machine Learning*, 2004.
- [37] A. Das, D. Kempe, Algorithms for subset selection in linear regression, in: *Proceedings of the fortieth annual ACM symposium on Theory of computing*, ACM, 2008, pp. 45–54.

- [38] B. Schölkopf, A. J. Smola, Learning with Kernels, MIT Press, 2001.
- [39] J.-L. Reyes-Ortiz, L. Oneto, A. SamÁ, X. Parra, D. Anguita, Transition-aware human activity recognition using smart-phones, Neurocomputing (2015).
- [40] Y. LeCun, L. Bottou, Y. Bengio, P. Haffner, Gradient-based learning applied to document recognition, in: Proceedings of the IEEE, Vol. 86, 1998, pp. 2278–2324.
- [41] N. Dalal, B. Triggs, Histograms of oriented gradients for human detection, in: 2005 IEEE Computer Society Conference on Computer Vision and Pattern Recognition (CVPR'05), Vol. 1, IEEE, 2005, pp. 886–893.
- [42] D. M. W. Powers, Evaluation: From precision, recall and f-measure to roc., informedness, markedness & correlation, Journal of Machine Learning Technologies 2 (1) (2011) 37–63.
- [43] J. Ott, E. Hyytiä, P. E. Lassila, J. Kangasharju, S. Santra, Floating content for probabilistic information sharing, Pervasive and Mobile Computing 7 (6) (2011) 671–689. doi:10.1016/j.pmcj.2011.09.001.
URL <http://dx.doi.org/10.1016/j.pmcj.2011.09.001>